

## I. PRELIMINARIES: THE STANDARD MODEL OF PARTICLE (ASTRO) PHYSICS

SM gauge group  $G_{\text{SM}} = \text{SU}(3) \times \text{SU}(2) \times \text{U}(1)$  mediated by gauge fields  $G_\mu^a$ ,  $W_\mu^i$ ,  $B_\mu$ , respectively (with field strength tensors  $G_{\mu\nu}^a$ ,  $W_{\mu\nu}^i$ ,  $B_{\mu\nu}$ ). Spontaneously broken to  $\text{SU}(3) \times \text{U}(1)_{\text{EM}}$  (mediated by  $G_\mu^a$  and  $A_\mu$ ) by VEV of Higgs doublet  $H(1, 2)_{+\frac{1}{2}}$ . Fermion matter, specified in terms of left-handed Weyl spinors  $q(3, 2)_{+\frac{1}{6}}$ ,  $u^c(\bar{3}, 1)_{-\frac{2}{3}}$ ,  $d^c(\bar{3}, 1)_{+\frac{1}{3}}$ ,  $l(1, 2)_{-\frac{1}{2}}$ ,  $e^c(1, 1)_{+1}$ . Renormalizable Lagrangian density<sup>1</sup>:

$$\mathcal{L} = \mathcal{L}_K - V_Y - V_0(H), \quad (1)$$

where

$$\begin{aligned} \mathcal{L}_K &= |\mathcal{D}^\mu H|^2 + i\bar{q}\bar{\sigma}^\mu \mathcal{D}_\mu q + i\bar{u}^c\bar{\sigma}^\mu \mathcal{D}_\mu u^c + i\bar{d}^c\bar{\sigma}^\mu \mathcal{D}_\mu d^c + i\bar{l}\bar{\sigma}^\mu \mathcal{D}_\mu l + i\bar{e}^c\bar{\sigma}^\mu \mathcal{D}_\mu e^c \\ &\quad - \frac{1}{4}B_{\mu\nu}B^{\mu\nu} - \frac{1}{4}W_{\mu\nu}^iW^{i\mu\nu} - \frac{1}{4}G_{\mu\nu}^aG^{a\mu\nu}, \end{aligned} \quad (2)$$

$$V_Y = -y_u H^T \epsilon q u^c + y_d H^\dagger q d^c + y_l H^\dagger l e^c + cc, \quad (3)$$

$$V_0(H) = m^2 |H|^2 + \lambda |H|^4. \quad (4)$$

Here  $\epsilon_{12} = -\epsilon_{2,1} = 1$ , and  $\mathcal{D}_\mu = \partial_\mu - igTF_\mu$ , summing on gauge groups with gauge couplings  $g$  and generators  $T$ . There are 3 generations of fermions, so  $y_{u,d,l}$  are 3x3 complex matrices.

Electroweak symmetry breaking (EWSB) is triggered by  $m^2 < 0$  (while  $\lambda > 0$ ) in Eq. (4), which causes the minimum of the potential to sit at  $|H|^2 = -m^2/(2\lambda)$ . It is convenient to deal with EWSB by explicitly splitting  $H$  into its components (denoted by EM charge),

$$H = \begin{pmatrix} G^+ \\ \frac{v+h}{\sqrt{2}} + iG^0 \end{pmatrix}. \quad (5)$$

EWSB is implemented via

$$\langle H \rangle = \begin{pmatrix} 0 \\ \frac{v}{\sqrt{2}} \end{pmatrix}. \quad (6)$$

The Goldstone bosons  $G^+$  (a complex scalar field) and  $G^0$  (a real pseudoscalar field) become the longitudinal modes of  $W^+$  and  $Z$ . In the same basis,

$$q = \begin{pmatrix} u^{+\frac{2}{3}} \\ d^{-\frac{1}{3}} \end{pmatrix}, \quad l = \begin{pmatrix} \nu \\ l^- \end{pmatrix}. \quad (7)$$

The Yukawa terms contain fermion masses,

$$V_Y = m_u q u^c + m_d q d^c + m_l l e^c + cc, \quad (8)$$

with  $m_u = \frac{y_u v}{\sqrt{2}}$ ,  $m_d = \frac{y_d v}{\sqrt{2}}$ ,  $m_l = \frac{y_l v}{\sqrt{2}}$ .

<sup>1</sup> I mostly follow the conventions of Dreiner, Haber, and Martin's arXiv:0812.1594 (DHM), apart from defining  $\bar{\psi} \equiv \psi^\dagger$  for conjugate 2-spinors. I keep (above, implicitly) DHM's descending index/ascending dotted index notation, for example,  $\bar{\psi}\bar{\sigma}^\mu\chi = \psi_\alpha^\dagger \bar{\sigma}^{\mu\dot{\alpha}\beta} \chi_\beta$ .

Gauge boson masses come from the covariant derivative, e.g.

$$|\mathcal{D}^\mu H|^2 \supset \left| \frac{g}{\sqrt{2}} \begin{pmatrix} 0 & W^{\mu+} \\ W^{\mu-} & 0 \end{pmatrix} \begin{pmatrix} 0 \\ \frac{v}{\sqrt{2}} \end{pmatrix} \right|^2 = m_W^2 W^{\mu+} W_\mu^- + \dots, \quad (9)$$

where  $m_W^2 = \frac{g^2 v^2}{4}$ .

Keeping only the VEV of  $H$  in the tree level potential leads to

$$V_0 \supset \frac{m^2}{2} v^2 + \frac{\lambda}{4} v^4. \quad (10)$$

As noted before, this is minimised at  $v^2 = -m^2/\lambda$ . The tree level mass of the physical Higgs particle is given by expanding  $V_0$  in powers of  $h$  around the minimum,

$$V_0 = -\frac{\lambda v^4}{4} + \frac{2\lambda v^2}{2} h^2 + \lambda v h^3 + \frac{\lambda}{4} h^4. \quad (11)$$

This yields the mass  $m_h^2 = 2\lambda v^2$ . Note how the linear term in  $h$  drops out.

Accelerator experiments have established the strength of the gauge coupling  $g \approx 0.65$ , and the particle masses  $m_W \approx 80$  GeV,  $m_t \approx 173$  GeV, and  $m_h \approx 125$  GeV. At tree level, we therefore have  $v = 2m_W/g \approx 246$  GeV, and can extract the parameters  $\lambda = m_h^2/(2v^2) \approx 0.13$  and  $y_t = \sqrt{2}m_t/v \approx 0.99$ .

In Eq. (1) we omitted a constant term in the Lagrangian. In QFT such constant term is harmless. But when GR is involved, a constant term is a cosmological constant and is not harmless. Later in this course we will come across the well-known appearance of the UV-sensitive contribution of quantum fluctuations to the cosmological constant. Even before that, though, it is interesting to consider how the picture of EWSB interplays with this problem, already at the classical level.

Fig. 1 illustrates the tree level picture of EWSB in the SM. We can read from Eq. (11) that the contribution of  $V_0$  to the cosmological constant is  $\rho_{\Omega,h} = -\frac{\lambda v^4}{4} \approx -(104 \text{ GeV})^4$ . This can be compared with the observed value  $\rho_\Lambda \approx (3 \times 10^{-3} \text{ eV})^4 = (3 \times 10^{-12} \text{ GeV})^4$ .

How does it happen that the constant pieces in the Lagrangian cancel each other so perfectly, to leave an almost vanishing cosmological constant right at the EW breaking minimum?

This may be even more puzzling when one notes that the structure of the QFT vacuum is generically quite rich. Indeed, the full structure of the SM Higgs vacuum – revealed when one includes quantum effects – is actually more interesting than the tree level picture suggests. Far away in field space, at  $\langle H \rangle \gg 10^{10}$  GeV, the SM Higgs potential admits another vacuum solution. Accelerator data suggests that the remote minimum is deeper than the local minimum we currently live in: we appear to be living in a *false vacuum*. The effective cosmological constant we'd experienced if the Universe tunnelled to the far away (true) vacuum state, would be large and negative!

## II. VACUUM STRUCTURE OF THE STANDARD MODEL HIGGS SECTOR

### A. Quantum structure of the Higgs sector: the effective potential

**The quantum effective action; 1-loop approximation; 1-loop effective potential (constant background field); functional determinants;  $\phi^4$  explicit example; relation to vacuum energy and zero-point fluctuations; relation to 1PI vertex functions; regularization and renormalization; RG-improved effective potential. The SM**

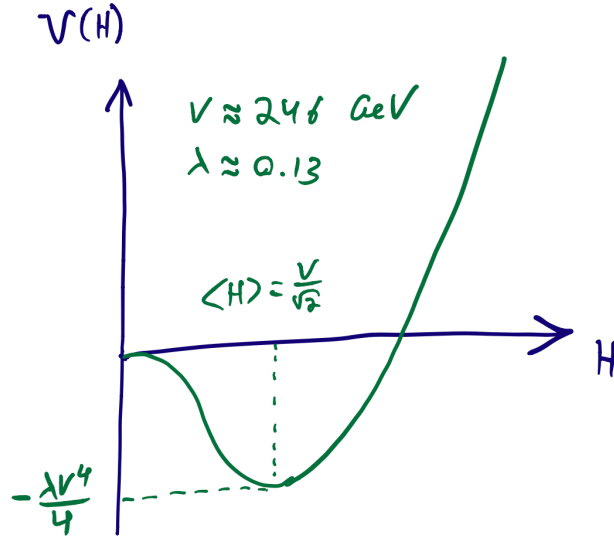


FIG. 1: SM tree level potential.

### 1-loop RG-improved effective potential; SM Higgs phase diagram; comparison to accelerator data, vacuum metastability.

The tree level structure of the SM Higgs potential is not too interesting. EWSB occurs with a negative  $m^2$  term and places the minimum of the potential at  $\langle H \rangle = -m^2/(2\lambda)$ . At larger field values, the potential shoots up like  $\lambda|H|^4$  with  $\lambda \approx 0.13$ .

We will now ask, what do quantum corrections do to this picture? Intuitively, one might think, not much... but that would actually be wrong: quantum effects turn out to trigger very interesting behaviour of the SM Higgs sector. This interesting behaviour happens not so much near the well-known EW vacuum we live in (which is affected, but not drastically or qualitatively); but rather, far away at large field space. The technical cause of these effects is essentially the large Yukawa coupling of the top quark: top quantum fluctuations enter the problem first at one loop, while being formally invisible at tree level. Thus, it may not be so surprising that quantum effects turn out to be qualitatively important: they pitch a new variable,  $y_t$ , into the game.

We will start the analysis with a quick derivation of the quantum effective action of a field theory, with sample computations in  $\phi^4$  theory. Then, we will deal with the full SM structure.

#### The quantum effective action; 1-loop approximation.

For simplicity, we will deal for a while with a real scalar field  $\phi$ . As a rule, spontaneous symmetry breaking (SSB) can be cast in terms of real scalar fields; more complicated theories just have more of these (the effects of fermions and vector bosons would be added indirectly).

What we are interested in, is to find the VEV of the field:

$$\langle \phi \rangle. \quad (12)$$

The path integral formalism allows us to compute such expectation values, using the external

source method. Consider the generating functional for connected Green's functions:

$$W[J] = -i\hbar \ln Z[J], \quad (13)$$

where

$$Z[J] = \mathcal{N} \int [D\phi] e^{\frac{i}{\hbar}(S[\phi] + \phi J)}. \quad (14)$$

Here  $S[\phi] = \int d^4x \mathcal{L}(\phi, \partial^\mu \phi)$ , and we use abbreviated notation with  $\phi J = \int d^4x \phi(x) J(x)$ . Connected correlation functions of the field are computed via

$$\langle \phi(x_1) \dots \phi(x_n) \rangle_J = \frac{\delta}{\delta J(x_1)} \dots \frac{\delta}{\delta J(x_n)} W[J]. \quad (15)$$

Specifically, the expectation value we are interested in can be obtained from:

$$\langle \phi(x) \rangle_J = \frac{\delta W[J]}{\delta J(x)} = \frac{\int [D\phi] \phi(x) e^{\frac{i}{\hbar}(S[\phi] + \phi J)}}{\int [D\phi] e^{\frac{i}{\hbar}(S[\phi] + \phi J)}} \equiv \bar{\phi}_J(x). \quad (16)$$

SSB occurs when  $\bar{\phi}_0 \neq 0$ .

It will be convenient to obtain  $\bar{\phi}$  as the field configuration that extremizes another functional,  $\Gamma[\bar{\phi}]$ , which is called the effective action. (We suppress the subscript  $J$  for a reason that will become apparent momentarily.)  $\Gamma[\bar{\phi}]$  is obtained from  $W[J]$  via a functional Legendre transform:

$$\Gamma[\bar{\phi}] = W[J] - J\bar{\phi}. \quad (17)$$

Here, we must consider  $J$  as a function of  $\bar{\phi}$  via the implicit solution of Eq. (16). That is, we now consider  $\bar{\phi}$  as the independent variable, with  $J$  derived from it by whatever value it needs to take to satisfy Eq. (16) with  $\bar{\phi}_J = \bar{\phi}$ . The functional derivative of  $\Gamma[\bar{\phi}]$  is easy to compute:

$$\frac{\delta \Gamma[\bar{\phi}]}{\delta \bar{\phi}} = \frac{\delta J}{\delta \bar{\phi}} \frac{\delta W}{\delta J} - \frac{\delta J}{\delta \bar{\phi}} \bar{\phi} - J = -J. \quad (18)$$

Therefore, the expectation value we are looking for is given by the field configuration  $\bar{\phi}$  that extremizes  $\Gamma[\bar{\phi}]$ , namely, for which  $\delta \Gamma[\bar{\phi}]/\delta \bar{\phi} = 0$ . As per Eq. (18), if we find such configuration, then it corresponds to  $J = 0$ .

We now calculate  $\bar{\phi}$  in the saddle point approximation. It is convenient to start with  $Z[J]$  directly.

Suppose we define  $\phi_c$  such that it solves the classical EOM, including the external source:

$$\left( \frac{\delta S[\phi]}{\delta \phi} + J \right)_{\phi=\phi_c} = 0. \quad (19)$$

Note that with this definition,  $\phi_c$  depends on  $J$ .  $\phi_c$  becomes the solution of the usual classical EOM in the limit  $J \rightarrow 0$ .

We can split the field as

$$\phi = \phi_c + \varphi. \quad (20)$$

In the limit  $J \rightarrow 0$ ,  $\varphi$  expresses quantum corrections to the classical SSB VEV. In a saddle point approximation, we expand:

$$Z[J] = e^{\frac{i}{\hbar}(S[\phi_c] + \phi_c J)} \int [D\varphi] e^{\frac{i}{2\hbar} \frac{\delta^2 S[\phi_c]}{\delta \phi_c^2} \varphi^2 + \dots}. \quad (21)$$

We will drop the next orders in  $\varphi$  (the ... terms). As a preliminary check, let us for a moment also drop the quadratic piece ( $\propto \varphi^2$ ) and consider only the  $\phi_c$  contribution. At this order in the expansion, we have  $Z[J] = e^{\frac{i}{\hbar}(S[\phi_c] + \phi_c J)}$ ,  $W[J] = S[\phi_c] + \phi_c J$ , and  $\Gamma[\phi_c] = W[J] - J\phi_c = S[\phi_c]$ . Thus, the tree level effective action is just the classical action, and  $\phi = \phi_c$  solves the classical EOM.

Next, we evaluate the Gaussian functional integral in Eq. (21). This gives a functional determinant:

$$\int [D\varphi] e^{\frac{i}{2\hbar} \frac{\delta^2 S[\phi_c]}{\delta \phi_c^2} \varphi^2} = \left[ \text{Det} \frac{-1}{2\hbar} \frac{\delta^2 S}{\delta \phi_c^2} \right]^{-\frac{1}{2}}. \quad (22)$$

Up to an additive constant, the corresponding correction to  $\Gamma[\phi_c]$  is, therefore,

$$\Gamma[\phi_c] = S[\phi_c] + \frac{i\hbar}{2} \ln \text{Det} \left( -\frac{\delta^2 S}{\delta \phi_c^2} \right). \quad (23)$$

Note that the effective action  $\Gamma[\phi_c]$  remains naturally a functional of the tree level classical field  $\phi_c$ , however, we have obtained a correction term which makes  $\Gamma[\phi_c] \neq S[\phi_c]$ . As a result, we expect that the quantum-corrected VEV  $\bar{\phi} \neq \phi_c$ .

**1-loop effective potential (constant background field); functional determinants;  $\phi^4$  explicit example; relation to zero-point fluctuations; relation to 1PI vertex functions.**

Let us evaluate Eq. (23) in  $\phi^4$  theory,

$$\mathcal{L} = \frac{1}{2} (\partial^\mu \phi)^2 - \frac{m^2}{2} \phi^2 - \frac{\lambda}{4} \phi^4 - \Lambda_0 \equiv \frac{1}{2} (\partial^\mu \phi)^2 - V_0. \quad (24)$$

We included a constant term  $\Lambda_0$ , which will play some role in the discussion later on. We find

$$-\frac{\delta^2 S}{\delta \phi_c^2} = \square + m_\phi^2 = \square + \frac{\partial^2 V_0(\phi_c)}{\partial \phi_c^2}, \quad (25)$$

where  $\square = \partial_t^2 - \vec{\nabla}^2$  and

$$m_\phi^2 = m^2 + 3\lambda\phi_c^2. \quad (26)$$

More in general, it is clear that  $-\delta^2 S/\delta \phi_c^2$  is the  $\phi_c$ -dependent inverse propagator of the theory. The functional determinant is evaluated by finding the eigenfunctions  $f_n(x)$  satisfying

$$(\square + m_\phi^2) f_n(x) = \lambda_n f_n(x). \quad (27)$$

Then  $\ln \text{Det} (\square + m_\phi^2) = \sum_n \ln \lambda_n$ .

Let us focus on the case in which  $\phi_c(x) = \phi_c$  independent of  $x$ ; that is, the VEV is constant in spacetime. This is the relevant case, if SSB does not also spontaneously break the translation invariance of the action.

The index  $n$  in Eq. (27) is continuous, and can be spanned by the 4-vector  $k = (k_0, \vec{k})$ . The eigenfunctions are  $f_n = f_k(x) = e^{ikx}$ , with eigenvalue  $\lambda_k = -k^2 + m_\phi^2 = -k_0^2 + \vec{k}^2 + m_\phi^2$ . This gives:

$$\frac{i\hbar}{2} \ln \text{Det} \left( -\frac{\delta^2 S}{\delta \phi_c^2} \right) = V_U \frac{i\hbar}{2} \int \frac{d^4 k}{(2\pi)^4} \ln \left( -k_0^2 + \vec{k}^2 + m_\phi^2 \right) \quad (28)$$

$$= -V_U \frac{\hbar}{2} \int \frac{d^4 k_E}{(2\pi)^4} \ln \left( k_E^2 + m_\phi^2 \right), \quad (29)$$

where  $V_U$  is the 4D volume of spacetime. In the second line we defined the Euclidean momentum,

$$k_E = (k_4, \vec{k}), \quad k_4 = -ik_0, \quad (30)$$

with which  $k_E^2 = k_4^2 + \vec{k}^2 = -k_0^2 + \vec{k}^2 = -k^2$ ,  $dk_0 = idk_4$ , and  $d^4k = id^4k_E$ .

A quick way to verify the continuum limit in Eq. (28), is to put space in a periodic box of size  $L$ . Let's do this in 1D for clarity. The eigenvalues are now discrete,  $k_n = \frac{2\pi n}{L}$ . The continuum limit is given by

$$\sum_n \ln \lambda_n = \sum_n \ln (k_n^2 + m_\phi^2) \rightarrow \int dn \ln (k_n^2 + m_\phi^2) = \frac{L}{2\pi} \int dk \ln (k^2 + m_\phi^2) \quad (31)$$

where  $dn = \frac{L}{2\pi} dk_n$  and we rename  $k_n \rightarrow k$ . In a 4D version of this argument we would get  $V_U = L^4$ .

Still assuming constant  $\phi_c$ , we can combine the tree level Lagrangian density with the quantum correction, and obtain

$$\Gamma[\phi_c] = \int d^4x \mathcal{L} - V_U \frac{\hbar}{2} \int \frac{d^4k_E}{(2\pi)^4} \ln (k_E^2 + m_\phi^2) \equiv -V_U V_{\text{eff}}, \quad (32)$$

$$V_{\text{eff}} = V_0 + V_1, \quad (33)$$

$$V_1 = \frac{\hbar}{2} \int \frac{d^4k_E}{(2\pi)^4} \ln (k_E^2 + m_\phi^2). \quad (34)$$

The SSB VEV, which is obtained from

$$\frac{\delta \Gamma[\phi]}{\delta \phi} = 0, \quad (35)$$

can be found by solving the minimisation equation

$$\frac{dV_{\text{eff}}(\phi)}{d\phi} = 0. \quad (36)$$

A few comments regarding the effective potential.

- $\phi$ -derivatives of the 1-loop effective potential  $V_{\text{eff}}$  generate 1-loop 1PI zero-momentum vertex functions of the theory describing quantum fluctuations around  $\phi = \phi_c$ , using the tree level potential  $V_0$ .

Let's make this explicit with an example, considering the 2-point vertex function in the  $\phi^4$  theory.

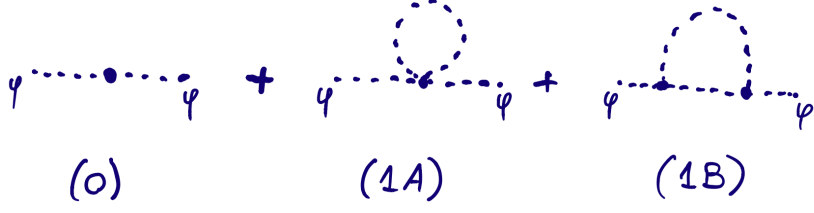
Again, express the tree level potential as a function of  $\phi = \phi_c + \varphi$ :

$$V_0(\phi_c + \varphi) = \frac{m^2}{2} (\phi_c + \varphi)^2 + \frac{\lambda}{4} (\phi_c + \varphi)^4 \quad (37)$$

$$= \frac{m^2}{2} \phi_c^2 + \frac{\lambda}{4} \phi_c^4 + (m^2 + \lambda \phi_c^2) \phi_c \varphi + \frac{m_\phi^2}{2} \varphi^2 + \lambda \phi_c \varphi^3 + \frac{\lambda}{4} \varphi^4. \quad (38)$$

We see immediately that the tree level mass of  $\varphi$  is  $m_\phi$ , and that the tadpole term  $\propto \varphi$  vanishes when computed at the tree level minimum  $\phi_c^2 = v^2 = -m^2/\lambda$ .

Let us compute the 1-loop 1PI 2-point vertex function,  $\mathcal{M}^{(2)}$ , of  $\varphi$  in this theory. We have the tree level diagram (0) and two 1-loop diagrams (1A and 1B), shown in Fig. 2. We find

FIG. 2: 2-point vertex function for  $\varphi$ .

$$i\mathcal{M}_{(0)}^{(2)} = -im_\phi^2, \quad (39)$$

$$i\mathcal{M}_{(1A)}^{(2)} = \frac{1}{2}4! \left( \frac{-i\lambda}{4} \right) \int \frac{d^4k}{(2\pi)^4} \frac{i}{k^2 - m_\phi^2 + i\epsilon} = 3\lambda \int \frac{d^4k}{(2\pi)^4} \frac{1}{k^2 - m_\phi^2 + i\epsilon}, \quad (40)$$

$$i\mathcal{M}_{(1B)}^{(2)} = \frac{1}{2}(3!)^2(-i\lambda\phi_c)^2 \int \frac{d^4k}{(2\pi)^4} \left( \frac{i}{k^2 - m_\phi^2 + i\epsilon} \right)^2 = \frac{1}{2}(6\lambda)^2\phi_c^2 \int \frac{d^4k}{(2\pi)^4} \frac{1}{(k^2 - m_\phi^2 + i\epsilon)^2}. \quad (41)$$

Rotating the integrals to Euclidean momentum,

$$\int \frac{d^4k}{k^2 - m^2 + i\epsilon} = -i \int \frac{d^4k_E}{k_E^2 + m^2}, \quad \int \frac{d^4k}{(k^2 - m^2 + i\epsilon)^2} = i \int \frac{d^4k_E}{(k_E^2 + m^2)^2}, \quad (42)$$

we obtain  $\mathcal{M}^{(2)} = \mathcal{M}_{(0)}^{(2)} + \mathcal{M}_{(1A)}^{(2)} + \mathcal{M}_{(1B)}^{(2)}$  given by

$$-\mathcal{M}^{(2)} = m_\phi^2 + \frac{6\lambda}{2} \int \frac{d^4k_E}{(2\pi)^4} \frac{1}{k_E^2 + m_\phi^2} - \frac{(6\lambda\phi_c)^2}{2} \int \frac{d^4k_E}{(2\pi)^4} \frac{1}{(k_E^2 + m_\phi^2)^2}. \quad (43)$$

Now, compare this result to direct derivative of the effective potential:

$$\begin{aligned} \frac{d^2 V_{\text{eff}}}{d\phi_c^2} &= m_\phi^2 + \frac{d^2}{d\phi_c^2} \frac{1}{2} \int \frac{d^4k_E}{(2\pi)^4} \ln(k_E^2 + m_\phi^2) \\ &= m_\phi^2 + \frac{6\lambda}{2} \int \frac{d^4k_E}{(2\pi)^4} \frac{1}{k_E^2 + m_\phi^2} - \frac{(6\lambda\phi_c)^2}{2} \int \frac{d^4k_E}{(2\pi)^4} \frac{1}{(k_E^2 + m_\phi^2)^2} \\ &= -\mathcal{M}^{(2)}, \end{aligned} \quad (44)$$

as promised.

Our explicit result for the 2-point 1PI vertex function applies similarly to all  $n$ -point functions. In other words,  $V_{\text{eff}}$  is the generating function of zero momentum 1PI vertex functions:

$$V_{\text{eff}}(\phi_c) = - \sum_{n=0}^{\infty} \frac{1}{n!} \phi_c^n \mathcal{M}^{(n)}. \quad (45)$$

- We obtained the 1-loop term  $V_1$  by performing the path integral over quantum fluctuations  $\varphi$  around the classical field  $\phi_c$ . One might expect that  $V_1$  can also be obtained by considering the vacuum energy density due to zero-point fluctuations, as found in canonical

quantization:

$$E_0 = \int \frac{d^3\mathbf{k}}{(2\pi)^3} \frac{\hbar\omega}{2} = \int \frac{d^3\mathbf{k}}{(2\pi)^3} \frac{\hbar}{2} \sqrt{\vec{k}^2 + m_\phi^2}. \quad (46)$$

In fact,  $V_1$  and  $E_0$  are equal up to a  $\phi$ -independent constant. To see this, note:

$$\frac{dE_0}{d\phi_c} = \frac{\partial m_\phi^2}{\partial \phi_c} \frac{\partial E_0}{\partial m_\phi^2} = \left( \frac{\partial m_\phi^2}{\partial \phi_c} \right) \frac{\hbar}{4} \int \frac{d^3\mathbf{k}}{(2\pi)^3} \frac{1}{\sqrt{\vec{k}^2 + m_\phi^2}}, \quad (47)$$

$$\frac{dV_1}{d\phi_c} = \frac{\partial m_\phi^2}{\partial \phi_c} \frac{\hbar}{2} \int \frac{d^3\mathbf{k}}{(2\pi)^3} \int \frac{dq}{2\pi} \frac{1}{q^2 + \vec{k}^2 + m_\phi^2} = \left( \frac{\partial m_\phi^2}{\partial \phi} \right) \frac{\hbar}{4} \int \frac{d^3\mathbf{k}}{(2\pi)^3} \frac{1}{\sqrt{\vec{k}^2 + m_\phi^2}}. \quad (48)$$

- It is interesting to fully reproduce the derivation of the effective potential via canonical quantization<sup>2</sup>. We will see this in TA. This method has a transparent generalisation beyond the “empty” vacuum background, i.e., when considering the system in a finite-temperature state, and we will revisit this point when we discuss finite- $T$  QFT.
- $V_1$  exhibits UV divergences, typical of 1-loop vertex functions. We need to regularise it and define the physical meaning of the parameters via renormalization conditions. The counterterms can be understood to reside in the 1-loop redefinition of the bare parameters  $\Lambda_0$ ,  $m^2$ , and  $\lambda$  in  $V_0$ .

### Regularization and renormalization; RG-improved effective potential.

We regularise  $V_1$  using dimensional regularisation. It is more convenient to work first with the derivative,

$$\frac{dV_1}{dm_\phi^2} = \frac{1}{2} \int \frac{d^4 k_E}{(2\pi)^4} \frac{1}{k_E^2 + m_\phi^2}. \quad (49)$$

Dim reg consists of deforming  $d = 4 - \epsilon$  and compensating the measure in momentum space via the introduction of a renormalisation scale  $\mu$ , as  $d^4 k_E \rightarrow \mu^\epsilon d^{4-\epsilon} k_E$ . We find

$$\begin{aligned} \frac{dV_1}{dm_\phi^2} &= \mu^\epsilon \frac{1}{2} \int \frac{d^{4-\epsilon} k_E}{(2\pi)^4} \frac{1}{k_E^2 + m_\phi^2} \\ &= \frac{\mu^\epsilon}{2(4\pi)^{2-\frac{\epsilon}{2}}} \frac{\Gamma(-1 + \frac{\epsilon}{2})}{\Gamma(1)} \left( \frac{1}{m_\phi^2} \right)^{-1 + \frac{\epsilon}{2}} \\ &= \frac{m_\phi^2}{2(4\pi)^2} \left( \frac{\epsilon}{2} \ln \frac{m_\phi^2}{4\pi\mu^2} - 1 \right) \left( 1 - \gamma_E + \frac{2}{\epsilon} \right). \end{aligned} \quad (50)$$

Integrating w.r.t.  $m_\phi^2$ , we obtain:

$$V_1(\phi_c) = \frac{m_\phi^4}{64\pi^2} \left( \ln \frac{m_\phi^2}{\mu^2} - \frac{3}{2} \right) + \frac{m_\phi^4}{64\pi^2} \left( \gamma_E - \ln 4\pi - \frac{2}{\epsilon} \right). \quad (51)$$

---

<sup>2</sup> See, e.g., Mukhanov, *Physical foundations of cosmology*, Ch.4.4.1.



To this, we should add the counterterms associated with the 1-loop redefinition of the bare parameters  $\Lambda_0$ ,  $m^2$ , and  $\lambda$  in  $V_0$ . The modified subtraction scheme ( $\overline{\text{MS}}$ ) amounts to defining these counterterms<sup>3</sup> such as to eliminate the term  $\propto (\gamma_E - \ln 4\pi - \frac{2}{\epsilon})$  in Eq. (51) (red part).

In what follows, we will refer by  $V_1$  to the regularised part in Eq. (51), that is, dropping the term  $\propto (\gamma_E - \ln 4\pi - \frac{2}{\epsilon})$ . Remember that our definition is specific to the  $\overline{\text{MS}}$  scheme, and the result obtained in other schemes (e.g. cut-off regularization) could differ by a different finite prefactor of the  $m_\phi^4$  term<sup>4</sup>.

The theory expressed via Eq. (51) is said to be defined at the RG scale  $\mu$ . The choice of  $\mu$  is arbitrary. Changing the numerical value of  $\mu$ , via  $\mu \rightarrow \mu'$ , would lead to a different parametrisation of the same theory; that is, such a change in  $\mu$  would be accompanied by a corresponding change in the parameters of the theory,  $\Lambda_0 \rightarrow \Lambda'_0$ ,  $m^2 \rightarrow m'^2$ ,  $\lambda \rightarrow \lambda'$ , done in precisely the right way so as to keep all physical objects fixed; where by physical objects we mean, e.g., particle pole masses, or scattering amplitudes.

To get some mileage out of this discussion, consider the 1-loop corrected VEV of the field. We denote this VEV by  $\bar{\phi} = v$  (recycling our def of  $v$  from the tree level discussion earlier). It is obtained by solving  $(dV_{\text{eff}}/d\phi)_{\phi=v} = 0$ . For  $m^2 < 0$ , we find:

$$v^2 = \frac{-m^2}{\lambda} \left( 1 - \frac{3\lambda}{8\pi^2} \left( \ln \frac{-2m^2}{\mu^2} - 1 \right) \right). \quad (52)$$

Now we have seen that the second derivative of the effective potential gives the 1-loop zero momentum 2-point function of field fluctuations  $\varphi$  around the classical background  $\phi_c$ . If we consider this as the 1-loop approximation for the  $\phi$  particle mass, call it  $M_\phi$ , and focus specifically on  $\varphi$  fluctuations around the physical VEV, we have:

$$-\mathcal{M}^{(2)} = M_\phi^2 = m_\phi^2 + \frac{d^2}{d\phi^2} \frac{m_\phi^4}{64\pi^2} \left( \ln \frac{m_\phi^2}{\mu^2} - \frac{3}{2} \right) \quad (53)$$

$$= -2m^2 \left( 1 + \frac{3\lambda}{16\pi^2} \left( \ln \frac{-2m^2}{\mu^2} + 2 \right) \right). \quad (54)$$

$M_\phi$  is a physical particle mass, and it cannot be changed by shifting the RG scale  $\mu$ . This gives us a quick derivation of how the parameter  $m^2$  must be adjusted, following a change in  $\mu$ . Specifically, we must impose:

$$\frac{dM_\phi^2}{d \ln \mu} = 0 = -2 \frac{\partial m^2}{\partial \ln \mu} + \frac{12\lambda m^2}{16\pi^2}. \quad (55)$$

Therefore, if we adjust  $\mu$ , then  $m^2$  is also adjusted by following the RG evolution:

$$\beta_{m^2} \equiv \frac{\partial m^2}{\partial \ln \mu} = \frac{3\lambda}{8\pi^2} m^2. \quad (56)$$

---

<sup>3</sup> Exercise: derive the counterterms. I find:

$$\delta\Lambda_0 = \frac{-m^4}{64\pi^2} \left( \gamma_E - \ln 4\pi - \frac{2}{\epsilon} \right), \quad \delta m^2 = \frac{-6\lambda m^2}{64\pi^2} \left( \gamma_E - \ln 4\pi - \frac{2}{\epsilon} \right), \quad \delta\lambda = \frac{-9\lambda^2}{64\pi^2} \left( \gamma_E - \ln 4\pi - \frac{2}{\epsilon} \right).$$

<sup>4</sup> In such other schemes, the physical meaning of the renormalised parameters  $\lambda$ ,  $m^2$ , etc. is different, but Green's functions evaluate to the same answer.

Above, we consistently retained only the 1-loop terms, neglecting the  $\mu$  dependence of  $m^2$  and  $\lambda$  in the 1-loop piece itself; these extra terms would be maintained in a 2-loop approximation.

We get a similar RGE for  $\lambda$ , considering the 4-point 1PI vertex. Let us call this vertex function  $\mathcal{G}$ :

$$-\mathcal{M}^{(4)} = \mathcal{G} = 6\lambda \left( 1 + \frac{9\lambda}{16\pi^2} \left( \ln \frac{-2m^2}{\mu^2} + 3 \right) \right). \quad (57)$$

We must impose,

$$\mu \frac{d\mathcal{G}}{d\mu} = 0 = 6 \frac{\partial \lambda}{\partial \ln \mu} - 6 \frac{18\lambda^2}{16\pi^2}. \quad (58)$$

The RGE of  $\lambda$  is then,

$$\beta_\lambda \equiv \frac{\partial \lambda}{\partial \ln \mu} = \frac{9\lambda^2}{8\pi^2}. \quad (59)$$

We can apply the same logic to the 0-point function, that is, the vacuum energy:

$$-\mathcal{M}^0 = \Lambda = \Lambda_0 - \frac{m^4}{4\lambda} \left( 1 - \frac{\lambda}{4\pi^2} \left( \ln \frac{-2m^2}{\mu^2} - \frac{3}{2} \right) \right). \quad (60)$$

Here,

$$\begin{aligned} \mu \frac{d\Lambda}{d\mu} = 0 &= \frac{\partial \Lambda_0}{\partial \ln \mu} - \frac{m^4}{8\pi^2} - \frac{\partial}{\partial \ln \mu} \left( \frac{m^4}{4\lambda} \right) \\ &= \frac{\partial \Lambda_0}{\partial \ln \mu} - \frac{m^4}{8\pi^2} - \frac{m^4}{4\lambda} \left( \frac{2\beta_m^2}{m^2} - \frac{\beta_\lambda}{\lambda} \right) = \frac{\partial \Lambda_0}{\partial \ln \mu} - \frac{m^4}{64\pi^2}. \end{aligned} \quad (61)$$

From this we see

$$\beta_\Lambda \equiv \frac{\partial \Lambda_0}{\partial \ln \mu} = \frac{m^4}{64\pi^2}. \quad (62)$$

As long as we keep the parameters  $\Lambda_0$ ,  $m^2$ , and  $\lambda$  on their RGE trajectories, we are guaranteed that all  $\phi$ -derivatives of the effective potential are  $\mu$ -independent. Of course, this means that  $V_{\text{eff}}$  is  $\mu$ -independent itself:

$$\frac{dV_{\text{eff}}}{d \ln \mu} = 0. \quad (63)$$

(To the 1-loop order at which we compute.)

Treating the theory parameters as “running parameters”, that is, tracking the RGE, allows us to consider any  $\mu$ . In fact, nothing stops us from considering:

$$\mu = \mu(\phi_c). \quad (64)$$

This freedom in choosing  $\mu$  becomes very useful at large field space, where  $\phi^2 \gg |m^2|$ . In this limit the effective potential becomes, approximately:

$$V_{\text{eff}}(\phi_c) \approx \frac{\lambda \phi_c^4}{4} \left( 1 + \frac{9\lambda}{16\pi^2} \ln \frac{3\lambda \phi_c^2}{\mu^2 e^{\frac{3}{2}}} \right). \quad (65)$$

The quantum correction is clearly expressed as the term in brackets. If we stick to a fixed constant  $\mu = \mu_0$ , we would eventually reach a region in  $\phi_c$  in which the quantum correction becomes large; this happens at  $\phi_c^2 \gtrsim \frac{\mu_0^2}{3\lambda} e^{\frac{16\pi^2}{9\lambda} + \frac{3}{2}}$ . At such large  $\phi_c$ , the 1-loop approximation cannot be trusted anymore.

However, we can bypass this difficulty, if we use the freedom in Eq. (64).

For instance, suppose we simply choose  $\mu^2 = m_\phi^2(\phi_c)e^{-\frac{3}{2}}$ . With this choice,  $V_1$  from Eq. (51) vanishes, and the quantum correction piece in  $V_{\text{eff}} = V_0 + V_1$  seems to vanish altogether! In particular, the large log at large  $\phi_c$  disappears.

In fact, the quantum correction did not disappear: implicitly, it is still at play. The point is that we must now treat  $\lambda$  as a running parameter:  $\lambda = \lambda(\mu(\phi_c))$ . The quantum correction manifests as a running of  $\lambda$ , via Eq. (59), which depends on  $\phi_c$  via  $\mu = \mu(\phi_c)$ . However, the large log *did indeed disappear*: our new effective potential expressed as the tree level potential with a running  $\lambda(\mu(\phi_c))$  is valid up to arbitrarily large  $\phi_c$ , as long as  $\lambda$  itself remains small and perturbative (in particular, as long as the 1-loop result for  $\beta_\lambda \propto \lambda^2$  remains parametrically more important than the omitted 2- and higher loop corrections, which scale as increasingly higher powers of  $\lambda$ ).

The effective potential defined via this smart use of the RGE is called the RG-improved effective potential. We will demonstrate the use of the RG-improved effective potential for the SM.

Before doing so, I should add a comment, regarding wave function renormalization. The RGE of couplings in the theory should be supplemented also by wave function renormalization, expressed via the anomalous dimension of the field,  $\gamma$ . This follows from the fact that the kinetic term of the field also evolves under the RGE. If we want the theory to express the dynamics of a canonically normalised field (with which we usually discuss particle excitations), we need to track this evolution. In the  $\lambda\phi^4$  theory, the anomalous dimension of  $\phi$  does not evolve, and wave function renormalization is absent. Once fermions and gauge bosons are put into the game, as in the SM, wave function renormalization must be included. It enters by replacing, in the effective potential,

$$\phi_c \rightarrow \xi(\mu)\phi_c, \quad (66)$$

$$\xi(\mu) = e^{-\int_0^t dt' \gamma(t')}, \quad t \equiv \ln \mu. \quad (67)$$

This replacement begins to be nontrivial only at first order in the loop expansion, so it needs to be included only for explicit factors of  $\phi_c$ , namely, in the  $m^2\phi_c^2$  and  $\lambda\phi_c^4$  terms. The impact of the wave function renormalization is a  $\phi_c$ -dependent stretching of  $V_{\text{eff}}$ ; for the examples we will study, the effect does not change qualitative results, and I leave the details of this analysis to the reader<sup>5</sup>.

### **The SM 1-loop RG-improved effective potential; SM Higgs phase diagram; comparison to accelerator data, vacuum metastability.**

To compute the SM effective potential, we need to supplement our theory with gauge and Yukawa interactions, and to extend the scalar sector from one real scalar to the SM SU(2) doublet  $H$  field. The derivation of the effective potential with extra scalar, fermion, and gauge d.o.f. follows similar lines to our single-scalar derivation: we just need to work out the functional

---

<sup>5</sup> A practical text to catch up on this topic (and other aspects of the effective potential) is Quiros, M., “Finite temperature field theory and phase transitions”, hep-ph/9901312.

determinants arising from these extra fields<sup>6</sup>. The result, in the  $\overline{\text{MS}}$  scheme, is:

$$V_1(\phi_c) = \sum_n N_n \frac{m_n^4}{64\pi^2} \left( \ln \frac{m_n^2}{\mu^2} - C_n \right). \quad (68)$$

Here, the index  $n$  sums over all of the d.o.f. of the theory; e.g.,  $n = h$  for the real neutral scalar component of the Higgs boson,  $n = t$  for the top quark,  $n = Z$  for the Z boson; etc. For each d.o.f.,  $m_n^2 = m_n^2(\phi_c)$  is the corresponding  $\phi_c$ -dependent particle mass. For example, for  $n = t$ , we have  $m_t^2 = \frac{y_t^2}{2} \phi_c^2$ , for  $n = W^\pm$  we have  $m_W^2 = \frac{g^2}{2} \phi_c^2$ , for  $n = Z$  we have  $m_Z^2 = \frac{g^2 + g'^2}{2} \phi_c^2$ , etc. To accommodate for the fact that our scalar is a complex SU(2) doublet, we choose a gauge basis in which:

$$H = \begin{pmatrix} G^+ \\ \frac{\phi_c + h}{\sqrt{2}} + iG^0 \end{pmatrix}. \quad (69)$$

This defines what we mean by the classical VEV  $\phi_c$ . Note that we must include the pseudoscalar Goldstone boson  $G^0$  and the complex Goldstone boson  $G^\pm$  in the sum on  $n$ .

The  $\overline{\text{MS}}$  constants  $C_n$  are given by  $C_n = 3/2$  for scalars and fermions, and  $C_n = 5/6$  for gauge bosons. The coefficients  $N_n$  count degrees of freedom. We have, for example,  $N_h = 1$  for  $n = h$ ,  $N_Z = 3$  for  $n = Z$ , and  $N_W = 2 \times 3 = 6$  for  $n = W^\pm$ . Note that we must count the d.o.f. in  $Z$  and  $W^\pm$  as 3 (per charge state), considering these fields as massive vectors. Importantly, the effective d.o.f. number for fermions has a negative sign: for  $n = t$ , this means  $N_t = -4 \times 3 = -12$ . Here, the factor of 4 accounts for the d.o.f. in a Dirac fermion, and the factor of 3 accounts for QCD index<sup>7</sup>.

Altogether, given the hierarchy between the different dimensionless SM couplings, the most important states to include at 1-loop are the top quark and the weak gauge bosons  $Z, W^\pm$ . Other bosons and fermions are subdominant. We can see this by the ratio of particle masses:  $m_t \approx 173$  GeV (compared to the next fermion in line,  $m_b \approx 4$  GeV), associated with the Yukawa coupling  $y_t \approx 1$ ;  $m_Z \approx 91$  GeV, and  $m_W \approx 80$  GeV, associated with the weak gauge couplings  $g \approx 0.65$ ,  $g' \approx 0.36$ .<sup>8</sup> Keeping only these most relevant states, we have

$$V_1(\phi_c) \approx -12 \frac{y_t^4 \phi_c^4}{256\pi^2} \left( \ln \frac{y_t^2 \phi_c^2}{2\mu^2} - \frac{3}{2} \right) + 6 \frac{g^4 \phi_c^4}{256\pi^2} \left( \ln \frac{g^2 \phi_c^2}{2\mu^2} - \frac{5}{6} \right) + 3 \frac{(g^2 + g'^2)^2 \phi_c^4}{256\pi^2} \left( \ln \frac{(g^2 + g'^2) \phi_c^2}{2\mu^2} - \frac{5}{6} \right). \quad (70)$$

To RG-improve this expression, we can set, for example:

$$\mu^2 = \exp \left\{ \frac{12y_t^4 \left( \ln \frac{y_t^2 \phi_c^2}{2} - \frac{3}{2} \right) - 6g^4 \left( \ln \frac{g^2 \phi_c^2}{2} - \frac{5}{6} \right) - 3(g^2 + g'^2)^2 \left( \ln \frac{(g^2 + g'^2) \phi_c^2}{2} - \frac{5}{6} \right)}{12y_t^4 - 6g^4 - 3(g^2 + g'^2)^2} \right\} \quad (71)$$

With this choice,  $V_1(\phi_c)$  vanishes from the effective potential. As discussed earlier, the quantum corrections now enter only via the RGE of the parameters  $\lambda$  and  $m^2$  in the tree level potential.

<sup>6</sup> See, e.g., Quiros, hep-ph/9901312.

<sup>7</sup> Even without doing the computation (which I recommend you do), the negative sign on  $N_n$  for fermions is easy to understand from the 1PI expansion of  $V_{\text{eff}}$  in Eq. (45). The structure of the 1-loop fermion contribution to  $\mathcal{M}^{(j)}$  is similar to that of the scalar contribution in  $\lambda\phi^4$ , but the fermion loop acquires the usual extra  $(-)$  sign w.r.t. the scalar loop.

<sup>8</sup> The Higgs scalar state itself (despite  $m_h \approx 125$  GeV) is not very important, with  $\lambda \sim 0.13$ .

Note that, at  $\phi_c = v \approx 246$  GeV, we have  $g \approx 0.65$ ,  $g' \approx 0.36$ ,  $y_t \approx 1$ , so the RHS of Eq. (71) is controlled by the top Yukawa coupling: for instance, the denominator is  $12y_t^4 - 6g^4 - 3(g^2 + g'^2)^2 \approx 12y_t^4(1 + 0.16)$ . This means that, effectively, our procedure roughly amounts to setting  $\mu(\phi_c) \approx m_t(\phi_c)$ . When we explore large values of  $\phi_c \gg v$ , however, the RGE of  $y_t$ ,  $g$ , and  $g'$  could in principle change this hierarchy. This actually does happen in the SM at large field, because the gauge coupling  $g'$  grows (approaching a Landau pole) while the Yukawa coupling  $y_t$  decreases due to the contribution of the QCD gauge coupling  $g_3$  in the  $y_t$  RGE.

To conclude, our 1-loop RG-improved SM effective potential is simply given by the SM tree level potential, with running parameters  $\lambda$  and  $m^2$ . To perform the computation, we need the  $\beta$  functions. The most important equations, which comprise a closed set, are:

$$\beta_\lambda \approx \frac{1}{(4\pi)^2} \left( 24\lambda^2 + \frac{9}{8}g_2^4 + \frac{27}{200}g_1^4 + \frac{9}{20}g_2^2g_1^2 - 9g_2^2\lambda - \frac{3}{5}g_1^2\lambda + 12y_t^2\lambda - 6y_t^4 \right), \quad (72)$$

$$\beta_{y_t^2} \approx \frac{y_t^2}{(4\pi)^2} \left( 9y_t^2 - 16g_3^2 - \frac{9}{2}g_2^2 - \frac{17}{10}g_1^2 \right), \quad (73)$$

$$\beta_{g_1^2} \approx \frac{41g_1^4}{5(4\pi)^2}, \quad (74)$$

$$\beta_{g_2^2} \approx \frac{-19g_2^4}{3(4\pi)^2}, \quad (75)$$

$$\beta_{g_3^2} \approx \frac{-14g_3^4}{(4\pi)^2}, \quad (76)$$

$$\beta_{m^2} \approx \frac{m^2}{(4\pi)^2} \left( 12\lambda + 6y_t^2 - \frac{9}{2}g_2^2 - \frac{9}{10}g_1^2 \right). \quad (77)$$

We anchor the RGE at  $\mu_0 = \mu(\phi_c = v) \approx m_t$ . The initial conditions are, approximately:

$$\begin{aligned} \lambda(\mu_0) &\approx 0.126, \quad m^2(\mu_0) \approx -(93 \text{ GeV})^2, \quad y_t(\mu_0) \approx 0.94, \\ g_1(\mu_0) &\approx 0.36\sqrt{\frac{5}{3}}, \quad g_2(\mu_0) \approx 0.65, \quad g_3(\mu_0) \approx 1.16. \end{aligned} \quad (78)$$

Here we made a change of variables, defining  $g_1 = \sqrt{(5/3)}g'$ . This is the convention for the hypercharge gauge coupling that naturally connects to analyses of a grand-unified theory (GUT); we will return to GUT at later chapters.

The solution with these initial conditions is shown in the left panel of Fig. 3. On the right we focus on  $\lambda$ .

The striking result is that  $\lambda$  decreases at large  $\phi_c$  and eventually drops below zero; at even larger field, the  $\beta$  function changes sign again, and  $\lambda$  stops decreasing, potentially exceeding zero again at super large field. A higher order computation confirms this picture, with minor corrections.

$\lambda$  dropping below zero signals vacuum instability; more precisely, as we shall see, metastability. The effective potential at tree level and at one loop is shown in Fig. 4. At small/intermediate field (left panel), the 1-loop quantum correction looks like a minor quantitative detailed effect. At large field, the instability is obvious: the SM effective potential exhibits a remote vacuum state at large field; our current EW vacuum state is merely a metastable configuration.

We would like to highlight that Fig. 3 shows a highly nontrivial situation: the vanishing of  $\lambda$  occurs not far from a zero of  $\beta_\lambda$ . In other words, the metastability of the SM vacuum is numerically marginal, a hit-and-run. A slight difference in the field content of the SM (and thus in the coupled set of  $\beta$  functions), or a slight change in the initial conditions of the couplings at the weak scale, could easily turn the metastability into either radical instability (with  $\lambda$  plunging

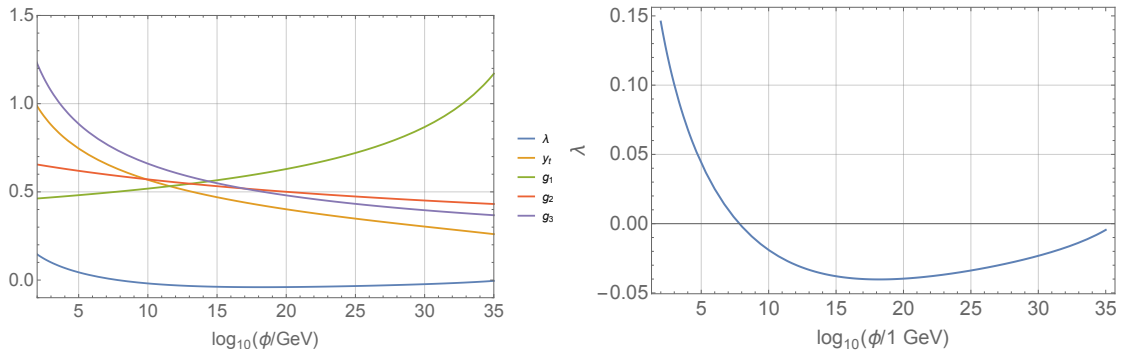


FIG. 3: Couplings RGE.

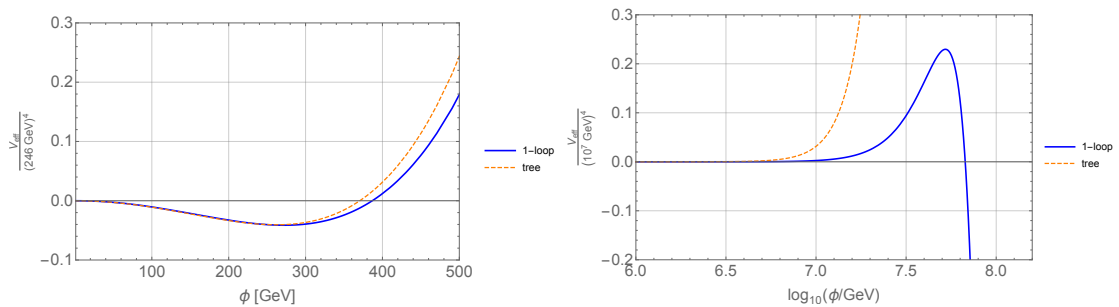


FIG. 4: SM effective potential.

deep below zero) or to complete stability (with  $\lambda$  never crossing zero). We illustrate this point with Fig. 5, from Andreassen, Frost, and Schwartz (2018).

The EW vacuum appears to be metastable against decay into a more stable vacuum configuration. This situation only makes sense from a cosmological perspective: if the Universe was infinitely old, metastability would be inconsistent with our EW existence. However, our Universe has a finite age. It is therefore potentially sensible that we live in the “wrong” vacuum; metastability could be consistent, if the Universe simply did not yet have enough time to tunnel away through the barrier separating the two vacua.

Naturally, our next goal is to understand this point better. What is the lifetime of a Universe trapped in the wrong vacuum?

### III. VACUUM METASTABILITY

**Vacuum decay in QM; vacuum decay in QFT; the bounce solution;  $\lambda\phi^4$  theory with  $\lambda < 0$ , explicit computation; rate of decay of the metastable SM vacuum.**

The effective action analysis of the previous section shows that we live in a metastable vacuum of the SM theory. How long are we expected to survive? Our goal in this section is to understand quantum phase transitions (tunnelling) in QFT, and apply this to the SM. We start with a recap of tunnelling in non-relativistic QM, in order to generate some

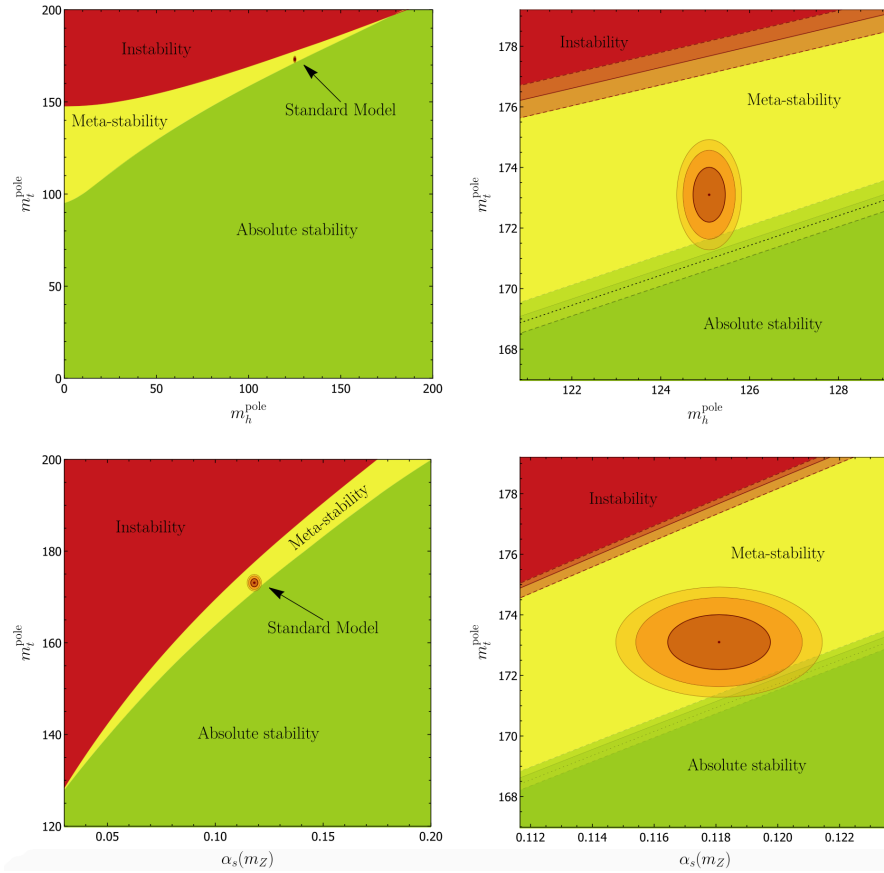


FIG. 5: Investigating the near-criticality of the SM vacuum. From Andreassen, Frost, and Schwartz, PRD97 056006 (2018).

intuition of the semi-classical approximation that we'll then apply to QFT and finally, to the SM.

### A. Vacuum decay in QM

It is illuminating to examine tunnelling by direct solution of the time dependent Schrodinger equation (SE), for some toy example. The solid line in the top-left panel of Fig. 6 shows a sample potential  $V(x)$  in a 1D QM problem. We initiate the wave function  $\psi(x, t)$ , shown by the thin red line, at  $\psi(x, 0) = \psi_0(x)$ . The potential was chosen such that  $V(x)$  is approximately a parabola near  $|x| \ll 1$ , and  $\psi_0$  was chosen as the lowest energy bound state solution of this parabola<sup>9</sup>. We

---

<sup>9</sup> Specifically, we take  $V(x) = (2x^2 - 0.75x^3 + 0.05x^4)/(1 + 0.025x^4)$ , so near the origin  $V(x) = 2x^2 + \mathcal{O}(x^3)$ . The approximate ground state is  $\psi_0 \propto e^{-x^2}$ , with energy  $E_0 \approx 1$ .

then solve the Schrodinger equation (SE) numerically (we set  $m = 1$ ):

$$i\partial_t\psi(x,t) = -\frac{1}{2m}\partial_x^2\psi(x,t) + V(x)\psi(x,t). \quad (79)$$

We define the false vacuum survival probability as

$$P = \int_a^b dx |\psi(x,t)|^2, \quad (80)$$

choosing  $-a = b = 1.5$ .

Fig. 6 shows the evolution of  $\psi$  and  $P$ . After some transient time,  $\psi$  enters a stage of steady

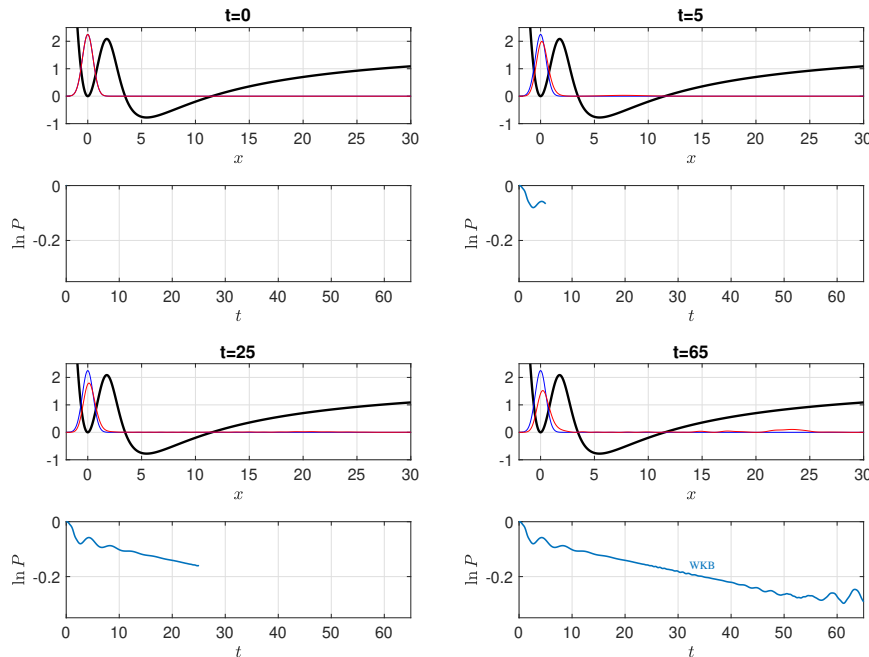


FIG. 6: Tunnelling in QM: numerical example. **Top:** Solid black: the potential. Thin blue: the initial wave function. Thin red: the evolving wave function. **Bottom:** Log of the survival probability  $P \equiv \int_{-1.5}^{1.5} dx |\psi(t)|^2$ . During the “WKB phase” we observe  $P \propto e^{-\Gamma t}$ .

exponential decay. Eventually, returning waves from the true vacuum perturb the decay of  $P$ . (In fact, if we track the evolution further, the return current of  $\psi$  begins to populate the false vacuum again.)

Note that the steady exponential decay  $P \approx e^{-\Gamma t}$  is associated with a steady probability current

$$j = \text{Im}\psi^* \partial_x \psi, \quad (81)$$

as  $\partial_t \ln P = -[j(b) - j(a)]/P \approx -\Gamma$ , where in the last approximation we assumed  $\Gamma t \ll 1$ .

The initial and late-time behaviour of  $P$  is interesting, but complicated, and we won’t attempt to analyse it here. Rather, we will focus on the exponential stage during which  $P \sim e^{-\Gamma t}$ . Let us solve analytically a simple square-well example.



1. *Direct computation in the Schrodinger approach: square-well potential*

Consider a square well potential,

$$V = \begin{cases} v, & x < -L, & \text{region L} \\ 0, & -L < x < L, & \text{region F} \\ v, & L < x < b, & \text{region B} \\ 0, & x > b, & \text{region R} \end{cases} \quad (82)$$

For concreteness, we start the wave function at the lowest energy bound state of the deformed problem in which  $V$  stays at  $v$  also for  $x > b$  (that is, eliminating region R). Up to normalisation, this initial state is given by

$$\psi_0 = \begin{cases} e^{\sqrt{2(v-w)}(x+L)}, & x < -L \\ \frac{1}{\cos(\sqrt{2w}L)} \cos(\sqrt{2w}x), & -L < x < L \\ e^{-\sqrt{2(v-w)}(x-L)}, & x > L \end{cases}, \quad (83)$$

where  $w$  is the smallest positive root of the equation

$$\sqrt{\frac{v-w}{w}} = \tan(\sqrt{2w}L). \quad (84)$$

Notice that in the infinite-barrier limit  $v \rightarrow \infty$  we have  $w \rightarrow \frac{\pi^2}{8L^2}$ , which is the usual infinite-well ground state energy. In practice we make sure that  $v > \frac{\pi^2}{8L^2}$ .

Once we deform the potential back into Eq. (82), the state begins to leak into region R. After a transient period, the decay rate relaxes into approximately constant  $\Gamma$ . The leaking state is stationary, up to the exponentially slow loss of probability. We show the evolution in Fig. 7.

We now show that this quasi-stationary leaking state solves the SE with a complex energy,  $w = w_0 - \frac{i}{2}\Gamma$ , and calculate  $\Gamma$ .

The boundary conditions describing the leaking state include a dominantly right-moving plane wave component that carries the flux of probability into region R. We therefore describe  $\psi$  in the different regions as follows:

$$\psi = \begin{cases} e^{\sqrt{2(v-w)}(x+L)}, & x < -L, & \text{region L} \\ f^+ e^{i\sqrt{2w}(x+L)} + f^- e^{-i\sqrt{2w}(x+L)}, & -L < x < L, & \text{region F} \\ b^+ e^{\sqrt{2(v-w)}(x-L)} + b^- e^{-\sqrt{2(v-w)}(x-L)}, & L < x < b, & \text{region B} \\ A e^{i\sqrt{2w}(x-b)}, & x > b, & \text{region R} \end{cases}. \quad (85)$$

Matching the L-F and F-B regions, we find

$$f^+ = \frac{1 - i\sqrt{\frac{v-w}{w}}}{2}, \quad f^- = \frac{1 + i\sqrt{\frac{v-w}{w}}}{2}, \quad (86)$$

$$b^+ = \left[ \frac{2\sqrt{w(v-w)}}{v \tan(2\sqrt{2w}L)} + \frac{v-2w}{v} \right] \frac{v \sin(2\sqrt{2w}L)}{2\sqrt{w(v-w)}}, \quad b^- = \frac{v \sin(2\sqrt{2w}L)}{2\sqrt{w(v-w)}}. \quad (87)$$

If there were no tunnelling (e.g., for  $b \rightarrow \infty$ ), then the bound state equation would amount to

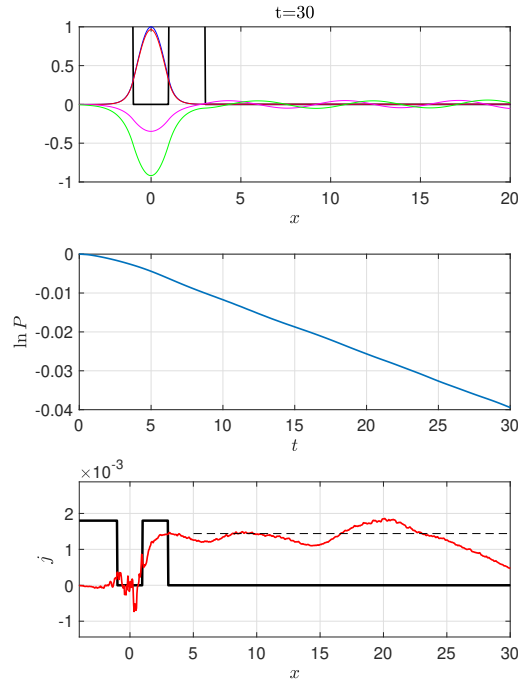


FIG. 7: Tunnelling in QM: square well example. Notice the outgoing flux in the bottom panel.

setting  $b^+ \rightarrow 0$ ,  $b^- \rightarrow 1$ . It can be seen that this is implied by Eq. (84)<sup>10</sup>.

But now, we also need to match the B-R regions:

$$b^+ = \frac{A}{2} \left( 1 + i \sqrt{\frac{w}{v-w}} \right) e^{-\sqrt{2(v-w)}(b-L)}, \quad b^- = \frac{A}{2} \left( 1 - i \sqrt{\frac{w}{v-w}} \right) e^{\sqrt{2(v-w)}(b-L)}. \quad (89)$$

The two sets of matching conditions for  $b^\pm$ , obtained for the F-B and B-R regions, would be

<sup>10</sup> If  $w$  satisfies Eq. (84), then

$$\begin{aligned} \frac{2\sqrt{w(v-w)}}{v \tan(2\sqrt{2wL})} &= \frac{2w \tan(\sqrt{2wL})}{v \tan(2\sqrt{2wL})} = \frac{2w \cos^2(\sqrt{2wL}) - \sin^2(\sqrt{2wL})}{v \cdot 2 \cos^2(\sqrt{2wL})} = \frac{w}{v} \left( 1 - \tan^2(\sqrt{2wL}) \right) \\ &= \frac{w}{v} \left( 1 - \frac{v-w}{w} \right) = -\frac{v-2w}{v}, \end{aligned} \quad (88)$$

and  $b^+$  vanishes as noted.

compatible if we could satisfy the following equations simultaneously:

$$A = \frac{2}{1 - i\sqrt{\frac{w}{v-w}}} \frac{v \sin(2\sqrt{2w}L)}{2\sqrt{w(v-w)}} e^{-\sqrt{2(v-w)}(b-L)}, \quad (90)$$

$$A = \frac{2}{1 + i\sqrt{\frac{w}{v-w}}} \frac{v \sin(2\sqrt{2w}L)}{2\sqrt{w(v-w)}} \left[ \frac{1}{\tan(2\sqrt{2w}L)} + \frac{v-2w}{2\sqrt{w(v-w)}} \right] e^{\sqrt{2(v-w)}(b-L)}. \quad (91)$$

Namely,

$$\begin{aligned} e^{-2\sqrt{2(v-w)}(b-L)} &= \frac{1 - i\sqrt{\frac{w}{v-w}}}{1 + i\sqrt{\frac{w}{v-w}}} \left[ \frac{1}{\tan(2\sqrt{2w}L)} + \frac{v-2w}{2\sqrt{w(v-w)}} \right] \\ &= \frac{\frac{v-2w}{v-w} - 2i\sqrt{\frac{w}{v-w}}}{\frac{v}{v-w}} \left[ \frac{1}{\tan(2\sqrt{2w}L)} + \frac{v-2w}{2\sqrt{w(v-w)}} \right]. \end{aligned} \quad (92)$$

Satisfying both real and imaginary parts of this equation requires that we complexify  $w$ ,

$$w = w_0 - \frac{i}{2}\Gamma. \quad (93)$$

Now we have two matching equations, and two variables,  $w_0$  and  $\Gamma$ , to solve them with. Expanding to leading order in  $\Gamma$ , the real and imaginary parts of the matching condition read:

$$\begin{aligned} e^{-2\sqrt{2(v-w_0)}(b-L)} &= \frac{v-2w_0}{v} \left[ \frac{1}{\tan(2\sqrt{2w_0}L)} + \frac{v-2w_0}{2\sqrt{w_0(v-w_0)}} \right] + \Gamma \frac{2\sqrt{\frac{w_0}{v-w_0}}}{\frac{v}{v-w_0}} \frac{\frac{4\sqrt{2}w_0L}{\sin^2(2\sqrt{2w_0}L)} + \frac{v^2}{(v-w_0)^{\frac{3}{2}}}}{8w_0^{\frac{3}{2}}}, \\ \Gamma e^{-2\sqrt{2(v-w_0)}(b-L)} \frac{(b-L)}{\sqrt{2(v-w_0)}} &= \frac{2\sqrt{\frac{w_0}{v-w_0}}}{\frac{v}{v-w_0}} \left[ \frac{1}{\tan(2\sqrt{2w_0}L)} + \frac{v-2w_0}{2\sqrt{w_0(v-w_0)}} \right] - \Gamma \frac{v-2w_0}{v} \frac{\frac{4\sqrt{2}w_0L}{\sin^2(2\sqrt{2w_0}L)} + \frac{v^2}{(v-w_0)^{\frac{3}{2}}}}{8w_0^{\frac{3}{2}}}. \end{aligned}$$

We look for a solution where  $\Gamma \sim e^{-\sqrt{2(v-w_0)}(b-L)}$ , and very small. Therefore to  $\mathcal{O}(\Gamma)$  we can throw the LHS of the last equation (note that the term in [...] is also very small: it relates to the exponentially small real correction to the ground state energy in region F, due to the runaway region R). With this approximation, after some work we find (simplifying the second equation):

$$\Gamma = \frac{8w_0^{\frac{3}{2}}}{\frac{4\sqrt{2}w_0L}{\sin^2(2\sqrt{2w_0}L)} + \frac{v^2}{(v-w_0)^{\frac{3}{2}}}} \frac{2\sqrt{w_0(v-w_0)}}{v-2w_0} \left[ \frac{1}{\tan(2\sqrt{2w_0}L)} + \frac{v-2w_0}{2\sqrt{w_0(v-w_0)}} \right]. \quad (94)$$

Plugging this into the first equation we can verify our assertion, that the term in [...] is exponentially small:

$$[...] = \frac{v-2w_0}{v} e^{-2\sqrt{2(v-w_0)}(b-L)}, \quad (95)$$

and plug it back in  $\Gamma$  to obtain:

$$\Gamma = \frac{16w_0^{\frac{3}{2}} \sqrt{w_0(v-w_0)}}{\frac{4\sqrt{2}w_0L}{\sin^2(2\sqrt{2w_0}L)} + \frac{v^3}{(v-w_0)^{\frac{3}{2}}}} e^{-2\sqrt{2(v-w_0)}(b-L)}. \quad (96)$$

This result is shown by the dashed line in the bottom panel of Fig. 7. It also agrees with the slope of  $\ln P$  in the middle panel. Finally, note that up to exponentially small corrections, setting  $[\dots] = 0$  amounts to  $w_0$  satisfying Eq. (84).

We conclude that the tunnelling solution converges into an approximate Hamiltonian eigenstate with complex energy, with an exponentially small imaginary part  $\Gamma$ . We found this in a painful, cumbersome way, by actually solving the SE. This strategy quickly becomes intractable beyond 1D and for realistic potentials.

It is good to remember that the approximate complex eigenstate we found, is really not a true exact eigenstate. All true eigenstates are purely real. We can be reminded of that by looking at Fig. 7: after spending some time in the steady-leaking state, one or both of two things happen: either the false vacuum is drained of probability, altering the solution; or returning flux from the true vacuum starts to refill the false vacuum, modifying the steady decay. Indeed, the way we derived the long lived – but transient – quasi-steady solution, was to slightly deform the full solution, such that – by hand – it contained just an outgoing plane wave in region R. This point would be very useful to recall in our next analysis. There, a similar deformation would be needed, albeit there it would be somewhat obscured in the path integral formalism.

## B. Path integral and Euclidean action for tunnelling in QM

Let us derive a new strategy for calculating  $\Gamma$ , that is easier to generalise to more complicated QM systems and also to QFT.

We can express the survival probability of the initial state by propagating it in time, then projecting it back onto itself:

$$a(t) = \langle \psi_0 | e^{-iHt} | \psi_0 \rangle. \quad (97)$$

With this,

$$P(t) = |a(t)|^2. \quad (98)$$

Focusing on the amplitude  $a(t)$ , we insert the energy eigenstates (we take these to span the continuum: we want states that contain outgoing waves in the analogue of region R),

$$a(t) = \int d\epsilon e^{-i\epsilon t} \rho(\epsilon), \quad (99)$$

where the positive spectral density  $\rho(\epsilon)$  is given by

$$\rho(\epsilon) = |\langle \epsilon | \psi_0 \rangle|^2. \quad (100)$$

Now, consider the amplitude  $a_E(\tau)$ , defined by analytically continuing  $a(t)$  to imaginary time,

$$t \rightarrow -i\tau; \quad (101)$$

namely,  $a_E(\tau) = a(t \rightarrow -i\tau)$ . We have:

$$a_E(\tau) = \int d\epsilon e^{-\epsilon\tau} \rho(\epsilon). \quad (102)$$

The Hamiltonian must have a ground state; let us say this has energy  $w$ . We can extract the ground state energy by taking the large  $\tau$  limit,

$$w = - \lim_{T \rightarrow \infty} \frac{1}{T} \ln a_E(T). \quad (103)$$

Now we make contact with the path integral formalism. Consider a particle initially situated at the bottom of the potential well, which we designate by  $x = 0$ . We also assume that the energy of the initial state is much smaller than the barrier; in the language of the previous example,  $w_0 \ll v$  (we make this requirement for simplicity, but in fact it should not be necessary: higher energy modes participating in the initial state would evaporate quickly, leaving the ground state behind). The amplitude for the particle to remain in the well for time  $T$  can be expressed by the path integral,

$$a(T) = \mathcal{N} \int [Dx] e^{iS[x]}. \quad (104)$$

It is convenient to choose the zero of time such that we consider the particle starting in the false vacuum at  $t = -\frac{T}{2}$  and ending in the false vacuum at  $t = \frac{T}{2}$ . Then,

$$S[x] = \int_{-\frac{T}{2}}^{\frac{T}{2}} dt \mathcal{L} \left( x(t), \frac{d}{dt} x(t) \right). \quad (105)$$

and the path integral contains all paths  $x$  that satisfy  $x(t = -\frac{T}{2}) = x(t = \frac{T}{2}) = 0$ .

The Euclidean amplitude reads

$$a_E(\tau) = \mathcal{N} \int [Dx] e^{-S_E[x]}, \quad (106)$$

where

$$\begin{aligned} -S_E[x] &= i \int_{-\frac{(-i)T}{2}}^{\frac{(-i)T}{2}} dt \mathcal{L} \left( x(t), \frac{d}{dt} x(t) \right) = \int_{-\frac{T}{2}}^{\frac{T}{2}} d\tau \mathcal{L}(x(\tau), i\dot{x}(\tau)) \\ &= - \int d\tau \left( \frac{\dot{x}^2}{2} + V \right) = - \int d\tau \mathcal{L}_E, \end{aligned} \quad (107)$$

in which we denote  $\dot{x} = \frac{dx}{d\tau}$ .

Combining Eqs. (103) and (106), we can extract the ground state energy from

$$w = - \lim_{T \rightarrow \infty} \frac{1}{T} \ln \mathcal{N} \int [Dx] e^{-S_E[x]}. \quad (108)$$

We will evaluate Eq. (108) in the steepest-descent approx. We are especially interested in contributions to the imaginary part of  $w$ . (A careful student should shout now: how are we going to get an imaginary part, from a manifestly real path integral?... Indeed, we are not. We will have to deform the path integral, in an analogous way to what we did when we enforced outgoing boundary conditions in the Schrodinger problem and complexify  $w$ .)

In steepest descent, we look for classical paths  $\bar{x}(\tau)$  in Euclidean time, which minimise  $S_E$ . By Eq. (107), the classical paths satisfy the EOM

$$\ddot{\bar{x}} = V'(\bar{x}). \quad (109)$$

This is identical to the EOM for a particle moving *in an inverted potential*.

A useful identity can be derived by noting that

$$\frac{d}{d\tau} \left( \frac{\dot{\bar{x}}^2}{2} - V \right) = \dot{\bar{x}} (\ddot{\bar{x}} - V') = 0. \quad (110)$$

Thus  $\frac{\dot{\bar{x}}^2}{2} - V = \text{Const}$ . It is convenient to set  $V(0) = 0$ , and then we see that  $\text{Const} = 0$ , so

$$\frac{\dot{\bar{x}}^2}{2} = V(\bar{x}). \quad (111)$$

This gives the useful property

$$\dot{\bar{x}} = \pm\sqrt{2V(\bar{x})}. \quad (112)$$

Thus we can write

$$S_E[\bar{x}] = \int d\tau 2V(\bar{x}(\tau)) = \int \frac{d\bar{x}}{|\dot{\bar{x}}|} 2V(\bar{x}) = \int d\bar{x} \sqrt{2V(\bar{x})}. \quad (113)$$

In the steepest descent, Gaussian approximation, we are left to compute

$$\mathcal{N} \int [Dx] e^{-S_E[x]} \approx e^{-S_E[\bar{x}]} \mathcal{N} \int [D\delta x] e^{-\frac{1}{2} S_E''[\bar{x}] \delta x^2}, \quad (114)$$

where  $\delta x(\tau)$  describes fluctuations around the classical path  $\bar{x}$ . If more than one distinct classical path exist, then we must sum the amplitude over all of them.

As usual, the operator  $S_E''[\bar{x}]$  is derived by expanding  $S_E[\bar{x} + \delta x]$  to 2nd order in  $\delta x$ , using integration by parts to convert  $(\dot{\delta x})^2 \rightarrow -\delta x \ddot{\delta x}$ . It is given by

$$S_E''[\bar{x}] \delta x^2 = \int d\tau \delta x [-\partial_\tau^2 + V''(\bar{x})] \delta x. \quad (115)$$

We expand  $\delta x$  in eigenfunctions of  $S_E''$ ,

$$\delta x(\tau) = \sum_\lambda \alpha_\lambda f_\lambda(\tau) \quad (116)$$

where

$$[-\partial_\tau^2 + V''(\bar{x})] f_\lambda(\tau) = \lambda f_\lambda(\tau). \quad (117)$$

It is convenient to normalise the eigenfunctions as

$$\int d\tau f_\lambda(\tau) f_{\lambda'}(\tau) = \delta_{\lambda, \lambda'}, \quad (118)$$

and to define the measure of the path integral as

$$\int [D\delta x] = \Pi_\lambda \int \frac{d\alpha_\lambda}{\sqrt{2\pi}}. \quad (119)$$

With this, we have

$$\mathcal{N} \int [D\delta x] e^{-\frac{1}{2} S_E'' \delta x^2} = \mathcal{N} \Pi_\lambda \int \frac{d\alpha_\lambda}{\sqrt{2\pi}} e^{-\frac{1}{2} \lambda \alpha_\lambda^2} = \mathcal{N} \Pi_\lambda \sqrt{\frac{1}{\lambda}} = \mathcal{N} \frac{1}{\sqrt{\text{Det} S_E''[\bar{x}]}}. \quad (120)$$

To proceed, we should ask: what classical paths can we find, with the boundary condition  $\bar{x}(-\infty) = \bar{x}(\infty) = 0$ ? Two solutions come to mind.

**The first solution simply stays at the peak of the (inverted) potential for all eternity:**  $\bar{x} = 0$ . This solution has zero action. To calculate the determinant, suppose that  $V'''(0) = \omega_0^2$ . The Euclidean vacuum-to-vacuum amplitude in the case  $V'''(0) = \omega_0^2$  is just the analytic continuation of the real-time vacuum-to-vacuum amplitude for the harmonic oscillator. The real-time amplitude for propagation from  $x_i$  at  $t = 0$  to  $x_f$  at  $t = T$  in the harmonic potential  $V(x) = \frac{\omega_0^2 x^2}{2}$  is<sup>11</sup>:

$$a^{(0)}(T) = \sqrt{\frac{\omega_0}{2\pi i \sin(\omega_0 T)}} e^{\frac{i\omega_0}{2\sin \omega_0 T} [(x_i^2 + x_f^2) \cos(\omega_0 T) - 2x_i x_f]} \xrightarrow{x_i=x_f=0} \sqrt{\frac{\omega_0}{2\pi i \sin(\omega_0 T)}}. \quad (121)$$

(The superscript (0) is to remind us that this is just the false vacuum contribution to the amplitude.) The Euclidean version of this is

$$a_E^{(0)}(T) = \sqrt{\frac{\omega_0}{2\pi i \sin(-i\omega_0 T)}} = \sqrt{\frac{\omega_0}{2\pi i \frac{e^{\omega_0 T} - e^{-\omega_0 T}}{2i}}} \rightarrow \sqrt{\frac{\omega_0}{\pi}} e^{-\frac{\omega_0 T}{2}}, \quad (122)$$

where in the end we took the limit of large  $T$ . Note that, as advocated, Eq. (108) gives the correct real part of the ground state energy – that is, the zero-point energy – of the harmonic oscillator problem; namely,  $\omega_0/2$ .

Using these results, we can determine the normalisation factor  $\mathcal{N}$  in terms of the false vacuum determinant:

$$\mathcal{N} = \sqrt{\frac{\omega_0}{\pi}} e^{-\frac{\omega_0 T}{2}} \sqrt{\text{Det} S_E''[0]}. \quad (123)$$

This will shortly become useful.

**A second solution is more interesting; it is called *the bounce*.** It starts at  $\bar{x}(-\infty) = 0$ , and begins to roll, very slowly, towards the valley region of the inverted potential (barrier of the real-time potential). It picks up speed in the valley, then slows down and eventually hits the classical turning point with zero velocity; it then turns around and goes back the same way it came, to rest back at  $\bar{x} = 0$  by  $\tau \rightarrow \infty$ . This back-and-forth behaviour is the reason for the name *bounce*. This solution is localised in time, and is a member of solutions of the classical field equations known as instantons. It is this solution that gives us the imaginary part we're after.

We denote the bounce solution by  $\bar{x}(\tau)_{\text{bounce}} = \bar{x}_b(\tau)$ . Note that the bounce action is positive,  $S_E[\bar{x}_b] > 0$ . This follows because the bounce is a nontrivial (that is, it necessarily sometimes have  $\dot{\bar{x}}_b \neq 0$ ) classical solution of the Euclidean EOM, so it satisfies Eq. (113), staying confined to the region where  $V \geq 0$ .

We must take special care for zero eigenvalues; in fact, there is indeed a zero mode: it is  $f_0(\tau) = A\dot{\bar{x}}_b(\tau)$ , where  $A$  is a normalisation factor. This is easy to see, using the EOM satisfied by  $\bar{x}_b$ , Eq. (109):

$$[-\partial_\tau^2 + V''(\bar{x}_b)] \dot{\bar{x}}_b(\tau) = -\partial_\tau (\ddot{\bar{x}}_b - V'(\bar{x}_b)) = 0, \quad (124)$$

The normalisation factor for this mode is

$$A = \frac{1}{\sqrt{\int d\tau \dot{\bar{x}}_b^2}} = \frac{1}{\sqrt{S_E[\bar{x}_b]}}, \quad (125)$$

---

<sup>11</sup> Feynman & Hibbs, Quantum mechanics and path integrals, problem 3.8.

namely,

$$f_0(\tau) = \frac{1}{\sqrt{S_E[\bar{x}_b]}} \dot{\bar{x}}_b(\tau). \quad (126)$$

The physical meaning of the zero mode is time-translation invariance: any solution of the form  $\bar{x}_b(\tau + \tau_0)$ , with  $\tau_0$  an arbitrary constant, is an equally good solution of the EOM with the same action as the original  $\bar{x}_b(\tau)$ , since the boundary conditions of the problem in Eq. (103) were pushed to infinity.

The zero mode pops out if we start from some  $\bar{x}_b(\tau)$  and shift it by an infinitesimal parameter  $\delta\tau$ , obtaining  $\bar{x}_b(\tau + \delta\tau) = \bar{x}_b(\tau) + dx(\tau) = \bar{x}_b(\tau) + \delta\tau \dot{\bar{x}}_b(\tau)$ . Thus, in evaluating the fluctuation integral we can simply factor out the zero mode, and explicitly integrate  $\delta\tau$  from  $-T/2$  to  $T/2$ :

$$\begin{aligned} \Pi_\lambda \int d\alpha_\lambda e^{-\frac{1}{2}\lambda\alpha_\lambda^2} &= \left[ \Pi'_\lambda \int d\alpha_\lambda e^{-\frac{1}{2}\lambda\alpha_\lambda^2} \right] \int \frac{d\alpha_0}{\sqrt{2\pi}} = \left[ \Pi'_\lambda \int d\alpha_\lambda e^{-\frac{1}{2}\lambda\alpha_\lambda^2} \right] \int \frac{d\delta\tau}{\sqrt{2\pi}} \left| \frac{d\alpha_0}{d\delta\tau} \right| \\ &= \left[ \Pi'_\lambda \int d\alpha_\lambda e^{-\frac{1}{2}\lambda\alpha_\lambda^2} \right] \int d\delta\tau \sqrt{\frac{S_E[\bar{x}_b]}{2\pi}} = T \sqrt{\frac{S_E[\bar{x}_b]}{2\pi}} \frac{1}{\sqrt{\text{Det}' S''_E[\bar{x}_b]}}, \end{aligned} \quad (127)$$

where by  $\text{Det}'$  we mean to delete the zero eigenvalue from the product of  $\lambda$  factors. We have used the Jacobian factor between  $\delta\tau$  integration and  $\alpha_0$  integration:

$$dx(\tau) = d\alpha_0 f_0(\tau) = \dot{\bar{x}}_b(\tau) d\delta\tau \quad \rightarrow \quad d\alpha_0 = \left( \frac{\dot{\bar{x}}_b}{f_0} \right) d\delta\tau = \sqrt{S_E[\bar{x}_b]} d\delta\tau. \quad (128)$$

Now comes an important point. We have found a zero mode of the fluctuation determinant, corresponding to  $f_0(\tau) = A\dot{\bar{x}}_b(\tau)$ . However, as discussed when we introduced the bounce, recall that  $\bar{x}_b$  starts its life at  $x = 0$ , rolls to the right through the potential barrier, and then slows down, stops, and rolls back to rest at  $x = 0$ . The crucial point is that during this motion,  $\dot{\bar{x}}_b$  necessarily flips sign! thus, the zero mode eigenfunction  $f_0(\tau)$  has a node. Necessarily, it is *not* the eigenfunction of lowest eigenvalue: there must exist at least another function  $f_{\lambda^-}$  for which  $\lambda^- < 0$ . I don't know how to prove it in general; but at least in typical circumstances, this negative eigenvalue can be shown to be unique, namely, all other eigenvalues are non-negative<sup>12</sup>.

The presence of a negative eigenvalue  $\lambda^- < 0$  makes the saddle point approximation produce a diverging factor:  $\int d\alpha_{\lambda^-} e^{|\lambda^-|\alpha_{\lambda^-}^2}$ . A way to circumvent this, is by analytically continuing the integral over  $\alpha_{\lambda^-}$  from the real axis into the complex plane. It is such analytic continuation that will give an imaginary part to the path integral.

This point is important, so we will dwell on it for some time: our path integral would be real, if it were not for an analytic continuation that we must perform to stabilise it. It is not a surprise, that the result is real unless we deform the computation (perhaps it is a little bit a surprise that this real result also blows up, but that's besides the point :-). The reason this happens, is that our formal computation was doomed from the get-go: the procedure in Eq. (103) was designed to pick up the ground state energy of the Hamiltonian; but true Hamiltonian eigenstates are stationary, not decaying anywhere; true Hamiltonian eigenvalues are real!

The solution to this difficulty is analogous to what we did in the brute force Schrodinger approach. There we enforced, by hand, an outgoing wave boundary condition in region R. No

---

<sup>12</sup> Some additional eigenvalues could be zero – representing additional symmetries of the action that are spontaneously broken by  $\bar{x}_b$  – of which we have a simple way to handle, similarly to what we did with time translation invariance.



true Hamiltonian eigenstate has this feature, because this state supported a net probability flux flowing outwards into R; the true, stationary, Hamiltonian eigenstate which would bear similarity to this would have a combination of incoming and outgoing waves in R, with no net flux. But the transient (although long-lived) decaying state we are after is really not an Hamiltonian eigenstate, and we really do want it to leak into R.

We must therefore deform the procedure of Eq. (103), in a way that would mimic the outgoing wave boundary condition in the Schrodinger method, and that would “fool” the  $\lim_{T \rightarrow \infty}$  Euclidean path integral into admitting a transient solution.

It should be clear by this time, that we could implement the deformation to obtain exponential decay by flux into R, but we could also just as well get exponentially slow population of the FV by incoming flux from R. The answer we would get, depends on how we perform the analytic continuation; that is, it depends on what sign we choose in letting  $\alpha_{\lambda^-} \rightarrow (\pm i)\tilde{\alpha}$  (with  $\tilde{\alpha}$  real).

At this point, we could try to jump ahead, and just rotate  $\alpha_{\lambda^-} \rightarrow (\pm i)\tilde{\alpha}$ , with  $\tilde{\alpha}$  real. This would produce  $\int_{-\infty}^{\infty} d\alpha_{\lambda^-} e^{|\lambda^-|\alpha_{\lambda^-}^2} \rightarrow (\pm i) \int_{-\infty}^{\infty} d\tilde{\alpha} e^{-|\lambda^-|\tilde{\alpha}^2} = (\pm i) \sqrt{\frac{2\pi}{|\lambda^-|}}$ . This is *almost* the correct answer: it is wrong only by a factor of  $\frac{1}{2}$ . The outcome of the path integral, where I introduce the missing factor of  $\frac{1}{2}$  (highlighting it for clarity) by hand for now, is:

$$\begin{aligned} a_E(T) &= \mathcal{N} \frac{1}{\sqrt{\text{Det}S''_E[0]}} + \frac{1}{2}(\pm i)\mathcal{N}T e^{-S_E[\bar{x}_b]} \sqrt{\frac{S_E[\bar{x}_b]}{2\pi}} \frac{1}{\sqrt{|\text{Det}'S''_E[\bar{x}_b]|}} \\ &= \sqrt{\frac{\omega_0}{\pi}} e^{-\frac{\omega_0 T}{2}} \left( 1 + \frac{1}{2}(\pm i)T e^{-S_E[\bar{x}_b]} \sqrt{\frac{S_E[\bar{x}_b]}{2\pi}} \sqrt{\frac{\text{Det}S''_E[0]}{|\text{Det}'S''_E[\bar{x}_b]|}} \right) \\ &= \sqrt{\frac{\omega_0}{\pi}} \exp \left\{ -T \left( \frac{\omega_0}{2} - \frac{1}{2}(\pm i) e^{-S_E[\bar{x}_b]} \sqrt{\frac{S_E[\bar{x}_b]}{2\pi}} \sqrt{\frac{\text{Det}S''_E[0]}{|\text{Det}'S''_E[\bar{x}_b]|}} \right) \right\} + \dots \quad (129) \end{aligned}$$

In going from the first line to the second, we used Eq. (123). In going from the second line to the third, we considered the exponentially small imaginary term  $\sim iT e^{-S_E[\bar{x}_b]}$  as the first term in the Taylor series of an exponential. Physically, this exponentiation describes the contribution to the path integral due to many bounces occurring in succession (Coleman & Callan '77).

One last time: there is nothing obviously wrong with either sign of the imaginary part; the choice between them must be guided by physics. The (+) sign corresponds to decay of the false vacuum into the R region; it is this sign we want in our computation of FV decay. The (−) sign corresponds to the opposite situation, population of an initially empty FV region via injection of flux from the R region.

Thus, we find:

$$\Gamma = -2\text{Im}\omega = 2\text{Im} \lim_{T \rightarrow \infty} \frac{1}{T} \ln a_E(T) = e^{-S_E[\bar{x}_b]} \sqrt{\frac{S_E[\bar{x}_b]}{2\pi}} \sqrt{\frac{\text{Det}S''_E[0]}{|\text{Det}'S''_E[\bar{x}_b]|}}. \quad (130)$$

In later analysis, we would be predominantly interested in the leading exponential suppression  $e^{-S_E[\bar{x}_b]}$ ; as we shall see,  $\mathcal{O}(1)$  (or, in fact, even orders of mag) corrections to the prefactor of the exponential term are not very important in practical cosmological considerations.

Now we return to the delicate factor of  $\frac{1}{2}$ . It is useful to visualise the analytic continuation procedure and its ingredients<sup>13</sup>.

<sup>13</sup> Recent discussion and references on this issue can be found in Andreassen, Farhi, Frost, and Schwartz, PRD95, 085011 (2017).

First, note that even without computing it in detail, we know quite a lot about the negative mode eigenfunction. In the Left panel of Fig. 8 we show the path  $x(\tau) = \bar{x}_b(\tau) + \alpha_{\lambda^-} f_{\lambda^-}(\tau)$ , for different values of  $\alpha_{\lambda^-}$ . Note that  $\alpha_{\lambda^-} = 0$  corresponds to the bounce itself, with action  $S_E[\bar{x}_b]$ . Now, we know that the negative mode eigenfunction has no nodes. This means that for  $\alpha_{\lambda^-} > 0$ , the path  $\bar{x}_b(\tau) + \alpha_{\lambda^-} f_{\lambda^-}(\tau)$  always extends above  $\bar{x}_b(\tau)$ , and vice-versa for  $\alpha_{\lambda^-} < 0$ . This property is seen in the paths in the left panel. In the right panel, we draw how these paths look like as trajectories superimposed on the inverted potential. (We also draw the actual potential, for reference, above.) For simplicity in the drawing, suppose that  $\alpha_{\lambda^-} = -1$  corresponds to the false vacuum static solution, which sits at  $x(\tau) = 0$  for all  $\tau$ . We assume this in the plot, but note that this is not essential for the discussion.

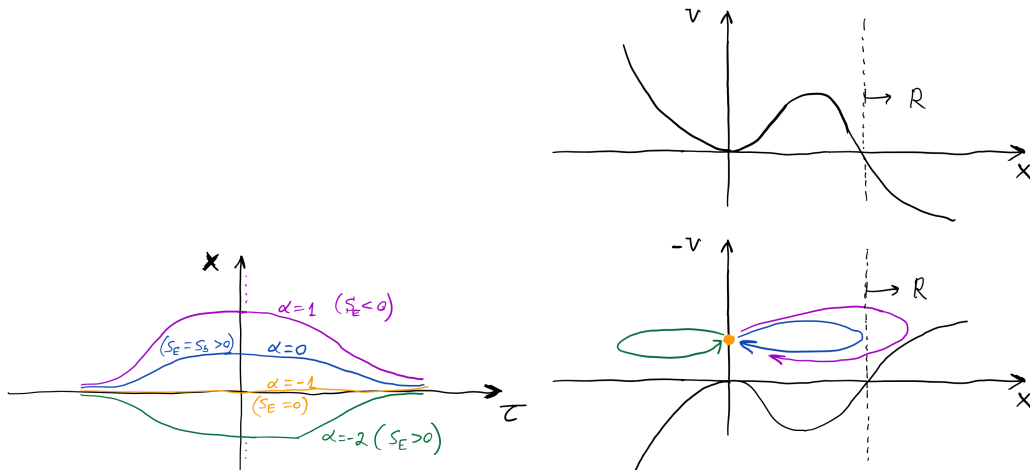


FIG. 8: Left: bounce, modified by the negative mode eigenfunction. Right: presented as paths on the potential landscape.

Next, how does the action look like for different values of  $\alpha_{\lambda^-}$ ? We show it in the left panel of Fig. 9. Let's explain. We know that the bounce action is positive,  $S_E[\bar{x}_b] > 0$ . And we know that  $f_{\lambda^-}$  is a negative mode eigenfunction, so for small excursions of  $\alpha_{\lambda^-}$  above or below zero,  $S_E$  must decrease below  $S_E[\bar{x}_b]$ . If we veer far into  $\alpha_{\lambda^-} < 0$ , we should eventually fall into the local minimum of  $S_E[0] = 0$ , the false vacuum. Going on towards deep negative  $\alpha_{\lambda^-}$  would see the action rise again, because  $\bar{x} = 0$ , again, is a minimum. It is clear why this is so: the  $\alpha_{\lambda^-} < 0$  paths remain in the stable region of the potential (green path in Fig. 8). They never feel a negative potential, and since the kinetic term in the action is positive, their total Euclidean action must be positive. Therefore, despite the negative eigenvalue, the region  $\alpha_{\lambda^-} < 0$  in the integral does not contribute to the functional determinant blowing up. That segment of the integral is convergent and manifestly real, so it would yield no imaginary part to the amplitude. It would just add an exponentially small correction to the real part of the exponent in Eq. (129).

In contrast, when we explore  $\alpha_{\lambda^-} > 0$ , the paths overshoot the classical turning point on the inverted potential. The moment we venture into the region to the right of the turning point, the path begins to explore negative values of  $V$ . If we increase  $\alpha_{\lambda^-}$  sufficiently, eventually we'll venture into negative  $S_E$ . It is only the negative  $S_E$  region in  $\alpha_{\lambda^-}$ -space, that causes the functional determinant to diverge. The  $\alpha_{\lambda^-} > 1$  paths overshoot the classical turning point, and stay for a long while in the true vacuum region, namely, region R from our earlier discussion. The return trip of these paths, back from region R into the the starting point near the false vacuum, represents precisely the returning flux that we wanted to eliminate. We need to stop

the return of these paths; this can be done by twisting the  $\alpha_{\lambda^-}$  integral into the complex plane, as illustrated in the right panel of Fig. 9<sup>14</sup>.

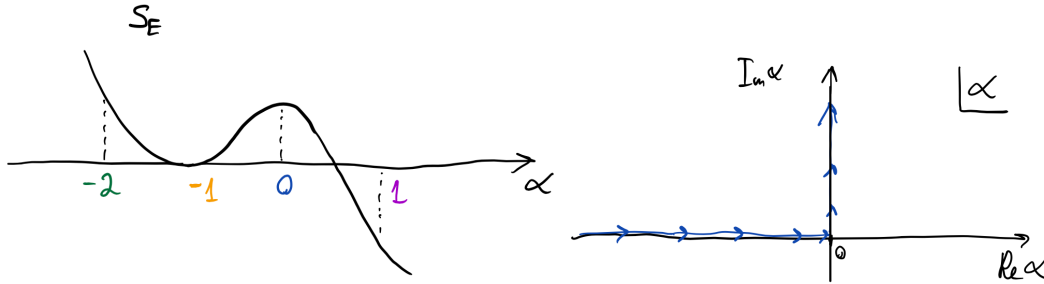


FIG. 9: Left: bounce action vs. the path parameter  $\alpha_{\lambda^-}$ . Right: the deformed (analytically continued) integral over  $\alpha_{\lambda^-}$ .

The fact that we only analytically continue the half-axis section  $\alpha_{\lambda^-} > 0$  in the integral over  $\alpha_{\lambda^-}$ , yields the factor of  $\frac{1}{2}$ , compared to what would obtain if we had simply Wick rotated the full range of  $\alpha_{\lambda^-}$ .

### C. Vacuum decay in QFT, and the metastable SM

#### Vacuum decay in QFT; the bounce solution.

The path integral derivation of vacuum decay in 1D QM generalises readily to  $D > 1$  and then  $D \rightarrow \infty$ , which becomes QFT upon the replacement  $\vec{x}(\tau) \rightarrow \phi(\vec{x}, \tau)$ . There are only two changes that we need to implement, in converting Eq. (130) to a QFT formula in  $D = 3 + 1$ :

1. The QM bounce corresponds in QFT to a classical solution of the Euclidean field EOM:  $\vec{x}_b(\tau) \rightarrow \bar{\phi}_b(x_E)$ , where  $x_E = (\tau, \vec{x})$  and  $\tau = it$ .
2. Instead of the single time-translation zero eigenmode we had in QM, there are now 4 eigenmodes corresponding to spacetime translations in  $D = 3 + 1$ . The modified determinant  $\text{Det}'$  corresponds to having all 4 zero eigenvalues deleted; at the same time, we obtain a spatial volume factor  $V$  from integrating over the spatial translations (in addition to the usual factor of  $T$  from integrating over the time translation, just as in QM).

With this understanding, the vacuum decay formula in QFT gives a decay rate per unit (spatial) volume<sup>15</sup>:

$$\frac{\Gamma}{V} = e^{-S_E[\bar{\phi}_b]} \frac{S_E^2[\bar{\phi}_b]}{(2\pi)^2} \sqrt{\frac{\text{Det} S_E''[0]}{|\text{Det}' S_E''[\bar{\phi}_b]|}} = \Lambda^4 e^{-S_E[\bar{\phi}_b]}. \quad (131)$$

<sup>14</sup> In Fig. 9 we distort the path up into positive imaginary  $\alpha_{\lambda^-}$ , leading to FV decay. Distorting into negative imaginary  $\alpha_{\lambda^-}$  would select the opposite process mentioned before.

<sup>15</sup> This can be interpreted as decay probability per unit spacetime 4-volume,  $\Gamma/V = p/(VT) = p/V_U$ .

For each of the 4 spacetime translation zero modes, we have a factor of  $\sqrt{S_E[\bar{\phi}_b]/(2\pi)}$ , leading to the over-all  $(S_E[\bar{\phi}_b]/(2\pi))^2$ . Finally, the functional determinants are given by the eigenvalue equation

$$[-\nabla_E^2 + V''(\bar{\phi}(x_E))] f_\lambda(x_E) = \lambda f_\lambda(x_E), \quad (132)$$

computed for the classical solutions  $\bar{\phi} = 0$  (the false vacuum) and  $\bar{\phi}_b$  (the bounce), where  $\nabla_E^2 = \partial_\tau^2 + \vec{\nabla}^2$ .

In practical applications of interest for cosmology, the non-exponential prefactor  $\Lambda^4$  of Eq. (131) is of relatively little importance. The units of this prefactor are [energy]<sup>4</sup>; setting  $\Lambda$  to some geometrical mean of the main energy scales in the problem – namely, the curvature of the potential near the false vacuum,  $\sqrt{V''(\bar{\phi}_0)}$ ; the characteristic scale of variation of the bounce,  $R^{-1} \sim \max \left| \frac{\nabla_E \bar{\phi}_b(x_E)}{\bar{\phi}_b(x_E)} \right|$ ; and so on – would only amount to logarithmic corrections to the exponential factor  $S_E[\bar{\phi}_b]$ . The main task is therefore to find  $\bar{\phi}_b$ , the bounce solution.

The bounce satisfies the EOM

$$\nabla_E^2 \bar{\phi}_b - \partial_\phi V(\bar{\phi}_b) = 0, \quad (133)$$

with boundary conditions  $\bar{\phi}_b(\tau \rightarrow \pm\infty, \vec{x}) = \bar{\phi}_0 = 0$ , that is, the bounce reduces to the false vacuum at past and future infinity, in all spatial directions. The minimum-action bounce is spherically symmetric<sup>16</sup> in Euclidean 4D, namely,  $\bar{\phi}_b = \bar{\phi}_b(\rho)$ , where  $\rho = \sqrt{\tau^2 + \vec{x}^2}$ . We will therefore assume  $\mathcal{O}(4)$  rotational invariance in what follows. The EOM simplifies to

$$\partial_\rho^2 \bar{\phi}_b + \frac{3}{\rho} \partial_\rho \bar{\phi}_b - \partial_\phi V(\bar{\phi}_b) = 0. \quad (134)$$

The boundary condition at infinity reduces to

$$\bar{\phi}_b(\infty) = 0. \quad (135)$$

In addition, we know that the bounce has a turning point, which we can define to occur at  $\tau = 0$ , at which  $\dot{\bar{\phi}}_b = 0$ . With  $\mathcal{O}(4)$  invariance, this turning point amounts to another boundary condition:

$$\partial_\rho \bar{\phi}_b(0) = 0. \quad (136)$$

This is sufficient data to find  $\bar{\phi}_b$ . We will perform a concrete calculation for  $\lambda\phi^4$  theory, which is relevant for understanding Higgs vacuum stability in the SM.

### **$\lambda\phi^4$ theory with $\lambda < 0$ , explicit computation; rate of decay of the metastable SM vacuum.**

As we have seen, the 1-loop effective potential of the SM is captured by the theory

$$V_{\text{eff}}(\phi) = \frac{m^2}{2} \phi^2 + \frac{\lambda}{4} \phi^4, \quad (137)$$

where quantum corrections manifest by having  $m^2 = m^2(\phi)$  and  $\lambda = \lambda(\phi)$ , obtained via the 1-loop RGE of  $m^2$  and  $\lambda$ , with initial values specified from accelerator data for  $\phi = v \approx 246$  GeV.

---

<sup>16</sup> Coleman, Glaser, and Martin, 88'; Blum et al, arXv:1611.04570.

Electroweak symmetry breaking is induced by  $m^2 < 0$  and  $\lambda > 0$  at the weak scale. The familiar EWSB vacuum state we live in therefore satisfies  $v^2 \approx -m^2(v)/\lambda(v)$ . However, also as we have seen, ours is merely a false vacuum: the negative running of  $\lambda$ , dominated by the top Yukawa coupling, leads to  $\lambda(\phi) < 0$  for some very large, but calculable and perturbative, field value,  $\phi \sim 10^8$  GeV. (At higher orders in perturbation theory, the numerical value of the zero-crossing of  $\lambda$  changes to somewhat larger field; however, the qualitative behaviour remains the same.)

At such large field values, above the zero crossing of  $\lambda$ , we can effectively neglect the  $m^2\phi^2$  term in the effective potential<sup>17</sup>. Up to the logarithmic running of  $\lambda$ , we can therefore approximate the potential for very large fields by

$$V_{\text{eff}}(\phi) \approx \frac{\lambda}{4}\phi^4, \quad (138)$$

where  $\lambda < 0$ , and where the false vacuum is approximated by the maximum at  $\phi \approx 0$ .

It may seem awkward to calculate a tunnelling rate in a potential of this form, because, after all, this potential has no barrier to speak of. However, this naive intuition is based on QM; it misses an interesting feature of the QFT problem. The point is that the action in QFT has the form

$$S_E[\phi] = \int d\tau \int d^3x \left( \frac{\dot{\phi}^2}{2} + \frac{(\vec{\nabla}\phi)^2}{2} + V(\phi) \right) = \int d\tau \int d^3x \left( \frac{\dot{\phi}^2}{2} + \tilde{V}(\phi) \right), \quad (139)$$

with  $\tilde{V} = V + \frac{1}{2}(\vec{\nabla}\phi)^2$ . It is  $\tilde{V}(\phi)$ , and not  $V(\phi)$ , which takes the role of the QM potential  $V(x)$ . The spatial derivative term acts as a kinetic barrier; it can (and does) render tunnelling exponentially suppressed, even if  $V(\phi)$  has no potential barrier in itself, to separate the false vacuum from the true.

Therefore, we push along, to find the bounce of the theory represented by Eq. (138). The bounce EOM is:

$$\partial_\rho^2 \bar{\phi}_b + \frac{3}{\rho} \partial_\rho \bar{\phi}_b - \lambda \bar{\phi}_b^3 = 0. \quad (140)$$

rescaling the coordinates via  $r = \sqrt{|\lambda|}\rho$ , we have  $\partial_r^2 \bar{\phi}_b + \frac{3}{r} \partial_r \bar{\phi}_b + \bar{\phi}_b^3 = 0$ , easily seen to be solved by  $\bar{\phi} = \sqrt{8\tilde{R}/(\tilde{R}^2 + r^2)}$  with an arbitrary parameter  $\tilde{R}$ . Rescaling back, we find the solution:

$$\bar{\phi}_b(\rho) = \sqrt{\frac{8}{|\lambda|} \frac{R}{R^2 + \rho^2}}. \quad (141)$$

Before we consider the physical meaning of the arbitrary parameter  $R$ , let us also compute the action for our solution. We find:

$$S_E[\bar{\phi}_b] = 2\pi^2 \int d\rho \rho^3 \left( \frac{1}{2} (\partial_\rho \bar{\phi}_b)^2 + \frac{\lambda}{4} \bar{\phi}_b^4 \right) = \frac{8\pi^2}{3|\lambda|}. \quad (142)$$

Notice that this result is independent of  $R$ . Also, as expected even for a barrier-less potential, QFT produces an exponentially-suppressed tunnelling action, due to the kinetic barrier.

We should clarify the meaning of the parameter  $R$ . As we have just verified,  $S_E$  is independent on the value of  $R$ : it is a flat direction, or in other words, represents yet another zero eigenmode

---

<sup>17</sup> **Exercise:** show that this is true, in the sense that the  $m^2\phi^2$  term is indeed numerically negligible compared with  $|\lambda|\phi^4$  for  $\phi$  even just slightly larger than the  $\lambda$  zero-crossing point.

in addition to the canonical spacetime translation set. The cause of the appearance of this zero eigenmode is a symmetry of the effective action, that is spontaneously broken by the bounce.

In the current case, the symmetry is scale invariance:  $\phi(x) \rightarrow \sigma\phi(\sigma x)$ , where  $\sigma$  is an arbitrary positive parameter. Indeed, the action is easily seen to be invariant under this transformation. In the Euclidean version we see that  $\int d\rho\rho^3\phi^4(\rho) \rightarrow \sigma^4 \int d\rho\rho^3\phi^4(\sigma\rho) = \int dy y^3\phi^4(y)$ , and  $\int d\rho\rho^3(\partial_\rho\phi(\rho))^2 \rightarrow \sigma^2 \int d\rho\rho^3(\partial_\rho\phi(\sigma\rho))^2 = \int dy y^3(\partial_y\phi(y))^2$ , so the potential and kinetic terms are separately invariant. The new zero eigenfunction is therefore, simply,  $\delta_\alpha\phi(\rho) = (1+\alpha)\phi((1+\alpha)\rho) - \phi(\rho) = \alpha(1+\rho\partial_\rho)\bar{\phi}_b(\rho)$ , which can be readily computed from  $\bar{\phi}_b$ .

Strictly speaking, we should define a collective coordinate and integrate over all values of  $R$ , just as we did for spacetime translations. However, in contrast to spacetime translation, the scale invariance of the effective theory is a mere artefact of the order in perturbation theory at which we have been working. Indeed, this can immediately be seen when we recall that  $\lambda(\phi)$  is in fact a running parameter, and not just a constant: that is, the RGE itself breaks the classical scale invariance of the  $\lambda\phi^4$  theory<sup>18</sup>.

More technical details of dealing with the approximate scale invariance are discussed in the literature; inevitably, as the scale invariance is an artefact of the 1-loop approximation, these details involve going beyond 1-loop in one way or another.

We bypass this discussion, with no big loss of accuracy, as follows. We simply estimate the decay rate of the SM Higgs vacuum by evaluating:

$$\frac{\Gamma}{V} \approx \max_\Lambda \left\{ \Lambda^4 e^{-\frac{8\pi^2}{3|\lambda(\Lambda)|}} \right\}, \quad (143)$$

where by  $\lambda(\Lambda)$  we use the running SM Higgs  $\lambda$  coupling along its RGE orbit (see the right panel of Fig. 3). Naturally, because of the dominance of the exponential factor, this expression for the decay rate is dominated by the region of  $\Lambda$  near where  $\beta(\Lambda)$  attains its minimum, that is, near the zero of the beta function  $\beta_\lambda(\Lambda)$ .

### True vacuum bubbles.

Now that we have this result, how do we understand its significance? Tunnelling in QM occurs when a particle from the FV region suddenly materializes on region R of the barrier. Upon popping in the region R, the particle commences to follow its classical EOM. Similarly, tunnelling in QFT occurs when the field in a localised region of space suddenly jumps from its  $\bar{\phi}_0 = 0$  FV value to a spacelike slice of the bounce,  $\bar{\phi}_b(\tau = 0, \vec{x})$ . Upon materialization, in an instant in (real) time that we can call  $t = 0$ , the field configuration is therefore a 3D spherical bubble with the profile  $\phi(t = 0, \vec{x}) = \phi_b(\sqrt{\vec{x}^2})$ . Having popped in the QFT analogue of region R, the field configuration commences to evolve following its classical real time (Minkowski) EOM.

In fact, given that the bounce has already given us the solution of the Euclidean EOM, an analytic continuation of the bounce,  $\bar{\phi}_b(\sqrt{\tau^2 + \vec{x}^2}) \rightarrow \bar{\phi}_b(\sqrt{-t^2 + \vec{x}^2})$ , automatically gives us a solution of the real time Minkowski EOM, which is simply an analytic continuation of the Euclidean version with  $\tau \rightarrow it$ . This solution is valid in the spacelike region  $\vec{x}^2 > t^2$ .

To visualise this, suppose that we have a SM-like bounce of the form Eq. (141), with some value of the parameter  $R$ . At the moment of nucleation of the bubble, say centred around the point  $\vec{x} = 0$ , the value of the field drops by a factor of 2 when we venture a distance  $|\vec{x}| = R$  in any direction. The 2-sphere surface of constant field then immediately begins to expand in

---

<sup>18</sup> Moreover, recall that in this analysis we also omitted the  $m^2\phi^2$  piece: this, too, breaks explicitly the would-be scale invariance of  $\lambda\phi^4$ .

space, tracing out the hyperbola

$$\bar{x}_{\frac{1}{2}}^2(t) = t^2 + R^2. \quad (144)$$

Within a time of order  $R$ , the front of the bubble is thus expanding at a speed quickly approaching the speed of light, converting as it goes false vacuum regions into true. In our computation above, the natural scale for  $R \sim \Lambda^{-1}$  was determined by the microscopical theory: if  $\Lambda$  is dominated by values where  $\beta_\lambda(\Lambda) \approx 0$ , then, from Fig. 3<sup>19</sup>,  $R \sim \Lambda^{-1} \sim (10^{17} \text{ GeV})^{-1} \sim 10^{-31} \text{ cm}$ . For all intents and purposes, therefore, the size of the bubble at its birth is cosmologically minuscule; the important point is that the bubble expands essentially at the speed of light, once it nucleated.

The metastability of the SM Higgs vacuum would therefore have cosmological consequences, if our past light cone contained one (or more) tunnelling events. Approximating the 4-volume of our past light cone by  $VT \sim 1/H_0^4$ , where

$$H_0 \approx 70 \frac{\text{km/s}}{\text{Mpc}} \approx \frac{70 \times 10^5}{3 \times 10^{24}} \frac{1}{\text{s}} \approx \frac{70 \times 10^5}{3 \times 10^{24}} \frac{2 \times 10^{-14}}{3 \times 10^{10}} \text{ GeV} \approx 1.5 \times 10^{-42} \text{ GeV} \quad (145)$$

is the current Hubble rate, we have that the cosmological condition for benign metastability (as opposed to catastrophic instability) is

$$\frac{\Gamma}{V} \frac{1}{H_0^4} \approx \max_\Lambda \left\{ e^{4 \ln \frac{\Lambda}{H_0} - \frac{8\pi^2}{3|\lambda(\Lambda)|}} \right\} < 1. \quad (146)$$

Namely, for any  $\Lambda$ , we must not have

$$-\lambda(\Lambda) > \frac{8\pi^2}{12 \ln \frac{\Lambda}{H_0}} \approx \frac{0.05}{1 + 0.08 \ln \left( \frac{\Lambda}{10^{15} \text{ GeV}} \right)}. \quad (147)$$

(Notice as an aside that changing the reference value of  $\Lambda$  from  $10^{15} \text{ GeV}$  to  $10^{10} \text{ GeV}$  would merely shift the instability criterion from  $|\lambda| \gtrsim 0.05$  to  $|\lambda| \gtrsim 0.063$ . This shows the extent to which the results are insensitive to the details of the pre-exponential factor.)

We can now appreciate the metastability of the SM in some more depth. The phase diagram of the SM Higgs sector can exhibit one of three qualitative scenarios:

1. Absolute stability: in this case, the EWSB vacuum we currently live in is absolutely stable. For this to be the case, quantum corrections to the effective action must not significantly destabilise the vacuum, and the RGE orbit of  $\lambda$  must not carry it below zero. In Fig. 5, the stable region of the theory is shown by the green area. The Higgs vacuum would be absolutely stable if, for example, the top quark mass (and thus, the top Yukawa coupling) is small, or if the Higgs particle mass at the local EWSB minimum (and thus, the initial condition of the running  $\lambda$ ) is large.
2. Metastability: in this case, quantum corrections lead to the formation of a remote minimum (in field space), that is deeper than our local EWSB minimum. Our current vacuum is thus unstable against tunnelling. However, since our Universe appears to have had only a finite lifetime so far, and thus a finite past light cone, it is conceivable that our local EWSB vacuum simply did not yet have enough time to decay into the energetically more favoured configuration. The metastability region is shown in Fig. 5 by the yellow band. It

---

<sup>19</sup> This radius becomes somewhat larger – and more comfortably distinct from the Planck length – when 2-loop corrections to the RGE of  $\lambda$  are included.

is a very narrow sliver in the SM parameter space; remarkably, we seem to reside precisely inside this sliver. This statement can be tested against particle physics data in terrestrial laboratory (accelerator) experiments. With  $\sim 95\%CL$ , we can say that we do in fact occupy a metastable state. Our 1-loop version of this computation agrees with this, as Fig. 4 shows that the running  $\lambda(\mu)$  does not cross  $-\lambda > 0.05$ . Detailed 2-loop computations agree as well.

3. Instability: in this case, the EWSB vacuum we live in should have already decayed into the remote minimum, within the current observed lifetime of the Universe. This is the red region in Fig. 5. Experimentally inferring SM parameters within the red region would render the theory observationally inconsistent, necessitating a new physics extension of the SM to stabilise the EWSB vacuum. For instance, note that the top quark mass  $m_t \approx 173$  GeV was known with reasonable accuracy a long time before the Higgs particle was detected (the top was discovered in 1995; the Higgs in 2012). A cosmological vacuum stability computation as in Fig. 5 could therefore have been used<sup>20</sup> to *predict*  $m_h \gtrsim 100$  GeV, almost two decades before the LHC discovery.

As I said, the observed parameters of the SM, determined from existing accelerator data, place the Universe at the metastable state. We didn't work out the tunnelling rate of this state in detail; doing so would require going into the nitty-gritty details of 2-loop RGE, to determine the precise behaviour of the running  $\lambda$ ; but, it is very slow, at least dozens of orders of magnitude above the current age of the Universe

## IV. HIGH-TEMPERATURE EFFECTS

### A. Symmetry restoration

**Finite-T effective potential; relation to Gibbs free energy; symmetry restoration; phase diagram and types of phase transitions; vacuum decay at high-T: QM thermal state barrier penetration, QFT computation; the SM at high-T.**

The SM Higgs vacuum state seems metastable. It is natural to ask, how did we come to occupy it, and not the true vacuum? One possibility is that the metastability is lifted by some new physics. Another is that there is no obvious reason why we should occupy one state and not the other: both are an equally fair choice, and ours just happens to also support life as we know it.

There is, however, an argument that may prefer our local vacuum over the remote one. It comes about when we consider the fact that the thermodynamic state of the Universe changes, when we scroll time and expansion backwards to very early times, and very high temperatures. As we will show in what follows, if we scroll backwards far enough, the ambient temperature and plasma pressure of the early Universe enter into the Higgs effective potential and deform it in such a way, as to single out a new vacuum state: the EW-conserving state, with  $\langle H \rangle = 0$ . This phenomenon is called symmetry restoration. It is quite generic and model-independent (albeit perhaps not completely model-independent). Starting the Universe from the EW symmetric state, and allowing it to expand and evolve towards its current cold and empty state, we find that our current metastable EW breaking local vacuum  $\langle H \rangle = v \sim 246/\sqrt{2}$  GeV is nearer to the

---

<sup>20</sup> See, e.g. M. Sher, "Electroweak Higgs Potentials and Vacuum Stability," Phys.Rept. 179 (1989) 273–418.



symmetric  $\langle H \rangle = 0$  starting point, and thus chronologically preferred compared to the remote, possibly stable, RGE-induced vacuum near the GUT scale.

Our goal in this section is to work out what happens to the Higgs effective potential when we calculate it not in an empty background, but rather in a background consisting of a high-temperature state of the SM d.o.f. This dynamics is important in cosmology; we will derive it in three complimentary ways: (i) thermodynamic considerations, (ii) canonical quantization, (iii) path integral.

### 1. Thermodynamic view of symmetry restoration

Up to a minus sign, the 1-loop Higgs effective potential,  $V_{\text{eff}}$ , is the part of the Lagrangian density which remains when we assume that  $\phi_c$  is constant in spacetime. We can thus incorporate the plasma contribution by adding to  $V_{\text{eff}}$  a term given by (minus) the background fluid Lagrangian density,  $\mathcal{L}_{\text{fluid}}$ . At high  $T$ , the plasma can be approximated by a hydrodynamical perfect fluid in thermal equilibrium. The on-shell effective Lagrangian density of a perfect fluid is given by the pressure:

$$\mathcal{L}_{\text{fluid}} = p. \quad (148)$$

The derivation of Eq. (148) is nontrivial<sup>21</sup>, and I do not provide it here (I will try to include it in subsequent versions of these notes). Using Eq. (148), the thermal correction to the effective potential is:

$$V_{\text{eff}} \rightarrow V_{\text{eff},T} = V_0 + V_1 + V_T, \quad (149)$$

$$V_T = -p. \quad (150)$$

The idea is to consider the plasma pressure  $p$  as function of  $\phi_c$  at fixed (or adiabatically slowly changing)  $T$ . The dependence of  $p$  on  $\phi_c$  enters via the dependence of plasma particle masses on  $\phi_c$ .

To shed some light on this calculation from thermodynamic considerations, consider the free energy density of the gas,

$$F = \rho - Ts. \quad (151)$$

This free energy density is relevant for a closed system, such as any segment of comoving volume in an homogeneous isotropic Universe. It is the part of the internal energy of the fluid that can be used to perform work during a thermodynamic process in which the temperature  $T$  of the system remains constant.

In thermodynamic equilibrium, the phase space density of a given d.o.f.  $i$  is given by (we neglect chemical potentials in this discussion)

$$f_i(k) = \frac{1}{e^{\beta\omega_k} \pm 1}, \quad (152)$$

with  $\omega_k = \sqrt{m_i^2 + \vec{k}^2}$ ,  $\beta = 1/T$ , and the sign  $\pm 1$  for fermions and bosons, respectively. With

---

<sup>21</sup> See Brown, J. D., *Class.Quant.Grav.* 10 (1993) 1579-1606 [gr-qc/9304026], and references therein.

this distribution function, the entropy density is given by<sup>22 23</sup>

$$s = \frac{\rho + p}{T}. \quad (153)$$

In this case, the free energy is  $F = -p$ , and we see that it coincides with  $V_T$ .

Let us work out the consequences of this procedure. The pressure contribution from each d.o.f. is

$$\begin{aligned} p_i &= \int \frac{d^3\mathbf{k}}{(2\pi)^3} f_i(k) \frac{\vec{k}^2}{3\omega} = \frac{1}{3} \int \frac{d^3\mathbf{k}}{(2\pi)^3} \frac{\vec{k}^2}{\sqrt{m_i^2 + \vec{k}^2}} \frac{1}{e^{\beta\sqrt{m_i^2 + \vec{k}^2}} \pm 1} \\ &= \frac{T^4}{6\pi^2} \int_0^\infty \frac{dx x^4}{\sqrt{\beta^2 m_i^2 + x^2}} \frac{1}{e^{\sqrt{\beta^2 m_i^2 + x^2}} \pm 1} \\ &= (\pm) \frac{T^4}{2\pi^2} \int_0^\infty dx x^2 \ln \left( 1 \pm e^{-\sqrt{\beta^2 m_i^2 + x^2}} \right). \end{aligned} \quad (154)$$

In the SM at high  $T$ , all of the particles are chiral, that is, all masses are proportional to the Higgs VEV. Considering the top quark, for example, we have  $m_t = y_t \phi_c / \sqrt{2}$ . The thermal term  $V_T = -p$  is plotted in Fig. 10, normalized to  $\frac{\pi^2 T^4}{90}$ . Near the origin of field space or at very high  $T$ , when  $\beta m \ll 1$ , we can expand Eq. (154) in powers of  $\beta m$ :

$$V_T^{\text{boson}} = g_i \left[ -\frac{\pi^2}{90} + \frac{\beta^2 m^2}{24} - \frac{(\beta^2 m^2)^{\frac{3}{2}}}{12\pi} - \frac{\beta^4 m^4}{64\pi^2} \ln \left( \frac{\beta^2 m^2}{a_B^2} \right) + \mathcal{O}((\beta m)^5) \right] T^4, \quad (155)$$

$$V_T^{\text{fermion}} = g_i \left[ -\frac{7\pi^2}{8 \cdot 90} + \frac{\beta^2 m^2}{48} + \frac{\beta^4 m^4}{64\pi^2} \ln \left( \frac{\beta^2 m^2}{a_F^2} \right) + \mathcal{O}((\beta m)^6) \right] T^4, \quad (156)$$

for bosons and fermions, respectively, with  $g_i$  d.o.f. per particle and with the constants  $a_B = 4\pi e^{\frac{3}{4} - \gamma_E}$ ,  $a_F = \pi e^{\frac{3}{4} - \gamma_E}$ .

- 
- <sup>22</sup> Derivation for fermions: the grand partition function is  $Z = \prod_i (1 + e^{-\beta\epsilon_i})$ , where  $i$  sums over single-particle microstates. In momentum space, we have  $\ln Z = \int \frac{d^3\mathbf{q}}{(2\pi)^3} \ln(1 + e^{-\beta\omega_q})$ . The entropy density is  $s = \frac{1}{V} \frac{\partial}{\partial T} \ln Z = -\int \frac{d^3\mathbf{q}}{(2\pi)^3} (\beta\omega_q(1 - f(\beta\omega_q)) + \ln f(\beta\omega_q))$ . As an aside, note that the entropy density can be written entirely in terms of  $f$  without direct reference to  $\omega_q$ . To see this, note that for  $f(x) = 1/(e^x + 1)$  we have  $\ln(1 - f) = x + \ln f$ , and  $f \ln f + (1 - f) \ln(1 - f) = x(1 - f) + \ln f$ , so  $s = -\int \frac{d^3\mathbf{q}}{(2\pi)^3} (\beta\omega(1 - f(\beta\omega)) + \ln f(\beta\omega)) = -\int \frac{d^3\mathbf{q}}{(2\pi)^3} (f \ln f + (1 - f) \ln(1 - f))$ . On the other hand, by integration by parts we can write  $p$  as  $p = T \int \frac{d^3\mathbf{q}}{(2\pi)^3} \ln(1 + e^{-\beta\omega}) = -T \int \frac{d^3\mathbf{q}}{(2\pi)^3} (\beta\omega + \ln f(\beta\omega))$ , while  $\rho = T \int \frac{d^3\mathbf{q}}{(2\pi)^3} f(\beta\omega)\beta\omega$ , so  $\frac{p+\rho}{T} = \int \frac{d^3\mathbf{q}}{(2\pi)^3} (\beta\omega f(\beta\omega) - \beta\omega - \ln f(\beta\omega)) = s$ .
- <sup>23</sup> Derivation for bosons:  $Z = \prod_i \frac{1}{1 - e^{-\beta\epsilon_i}}$ ,  $\ln Z = -\int \frac{d^3\mathbf{q}}{(2\pi)^3} \ln(1 - e^{-\beta\omega_q})$ ,  $s = \frac{1}{V} \frac{\partial}{\partial T} \ln Z = \int \frac{d^3\mathbf{q}}{(2\pi)^3} (\beta\omega_q(1 + f(\beta\omega_q)) + \ln f(\beta\omega_q)) = -\int \frac{d^3\mathbf{q}}{(2\pi)^3} (f \ln f - (1 + f) \ln(1 + f))$ . On the other hand, by integration by parts we have  $p = -T \int \frac{d^3\mathbf{q}}{(2\pi)^3} \ln(1 - e^{-\beta\omega}) = T \int \frac{d^3\mathbf{q}}{(2\pi)^3} (\beta\omega + \ln f(\beta\omega))$ , while  $\rho = T \int \frac{d^3\mathbf{q}}{(2\pi)^3} f(\beta\omega)\beta\omega$ , so  $\frac{p+\rho}{T} = \int \frac{d^3\mathbf{q}}{(2\pi)^3} (\beta\omega f(\beta\omega) + \beta\omega + \ln f(\beta\omega)) = s$ .

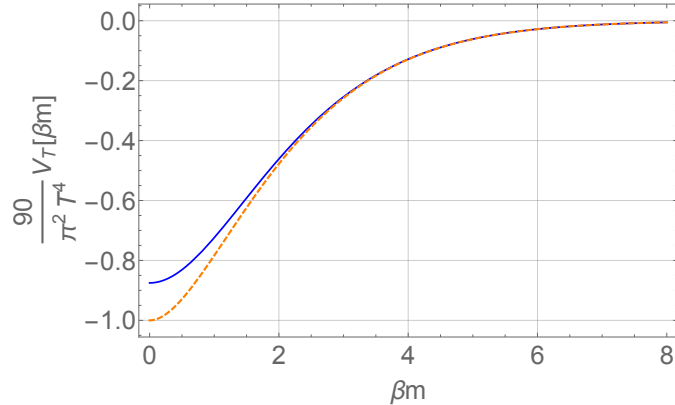


FIG. 10: Left: bounce action vs. the path parameter  $\alpha_{\lambda-}$ . Right: the deformed (analytically continued) integral over  $\alpha_{\lambda-}$ . Dashed line: bosons. Solid line: fermions.

The first term in Eqs. (155) and (156) is a constant in  $\phi_c$  space, so it does not directly affect the structure of the potential (it does indirectly affect the dynamics of SSB, because it enters the Hubble friction term in the scalar field EOM).

The second term in both of Eqs. (155) and (156) is a positive  $m^2 T^2$  term. Since  $m_i \propto \phi_c$  for the SM fermion and gauge boson states,  $V_T$  increases the stability of  $V_{\text{eff},T}$  near the origin  $\phi_c = 0$ . In fact, at very high  $T$  or near the origin of field space, the expansions above imply that the leading effect of  $V_T$  is to introduce a  $T$ -dependent positive correction to the effective mass term of  $\phi$ . (You can take a look at Eqs. (157) and (158), that we will come to momentarily.)

Fig. 11 demonstrates the stabilization effect. We show the total  $V_{\text{eff},T}$  for different values of  $T$ ; the lowest-lying curve corresponds to  $T = 0$ , and the subsequent higher curves have increasing values of  $T$ . We subtract a constant from all curves so they start at zero. On the left (right) panel, we show the result obtained when considering one boson (fermion) species of particle in the plasma, with  $g = 12$  and a mass term  $m = y\phi/\sqrt{2}$ , taking  $y = 1$ . The zero- $T$  part of the potential is taken as the tree-level Higgs potential (we know already that at small field space, this gives a reasonable approximation of the total 1-loop quantum potential).

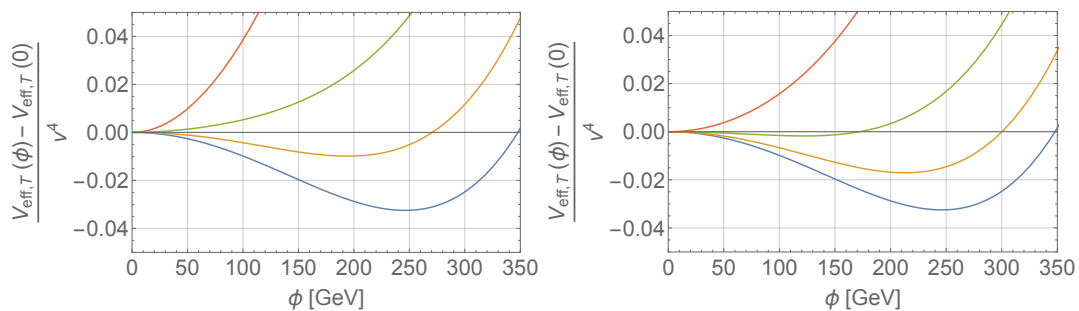


FIG. 11: SSB; different  $T$  curves correspond to different  $T$ , with the bottom curve at  $T = 0$  and higher curves with increasing  $T$ . Left: one boson species in the plasma. Right: one fermion species.

Fig. 11 demonstrates how the phenomenon of SSB plausibly happened in the SM. Viewing

the process backwards in time, at high  $T \gtrsim 100$  GeV the stabilizing effect of the SM background plasma pushed the minimum of  $V_{\text{eff},T}$  to  $\phi_c = 0$ : the EW symmetry was in tact. The symmetry is said to be *restored*. In the actual flow of time, at least during the minimal version of big-bang evolution, as the Universe expands and cools the EWB minimum – which was initially masked out by the plasma background – forms, as in Fig. 11. Eventually, the field slides into the EWB solution.

Precisely how SSB happens, as a dynamical process, depends on the details of  $V_{\text{eff},T}$  near the critical temperature  $T_c$ , defined as the value of  $T$  at which the symmetry-conserving solution  $\phi_c = 0$  ceases to be a global minimum. It is interesting to zoom-in the potential just at the moment  $T \approx T_c$ . We do this in Fig. 12.

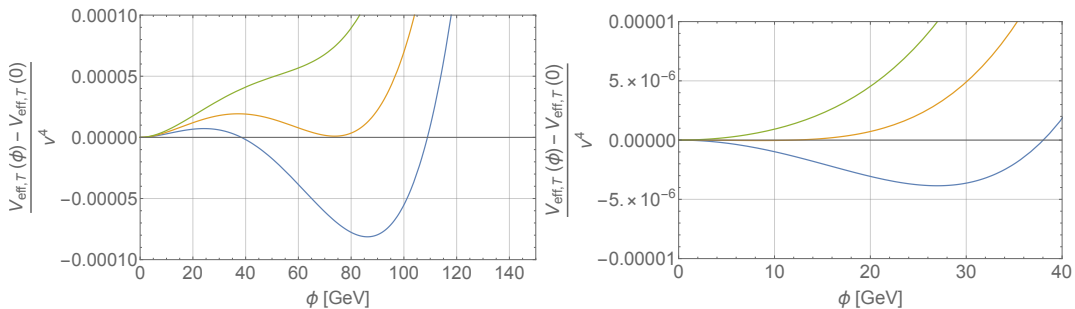


FIG. 12: A zoom-in view of Fig. 11 near the critical temperature  $T_c$ .

If the plasma is dominated by boson d.o.f., then at  $T \approx T_c$  a potential barrier forms between the symmetry-conserving minimum and the new SSB minimum. This is seen in the left panel of Fig. 12. We can understand the formation of the barrier by considering the third (cubic in  $m$ ) term in the small- $\beta m$  expansion, Eq. (155). It is interesting to note that the cubic term is a non-analytic function of  $\phi_c$  (or equivalently  $m_i$ ), as it corresponds to a piece  $\propto (\phi_c^2)^{\frac{3}{2}}$ . Such non-analyticity cannot arise at any finite order in Feynmann perturbation theory: from the perturbation theory point of view, it must (and indeed does) come from summing together an infinite set of Feynmann diagrams.

For fermions (right panel of Fig. 12), the cubic term is absent, and there is no barrier at  $T \approx T_c$ ; instead, the symmetry-conserving minimum smoothly disappears, continuously sliding to the right in field space.

As long as a potential barrier exists, SSB must proceed through barrier penetration. We have seen the zero- $T$  version of this process: it is a violent dynamical process of bubble nucleation. The high- $T$  version of the process is comparably interesting, and will be considered later on. If SSB proceeds in this violent way, the process is called a first order phase transition (PT).

If the transition is smooth, with no potential barrier, then the PT is expected to be smooth and can be homogeneous in space. This kind of transition is called second order.

Let us explore the dynamics of SSB within the SM. At high  $T$  and near the origin of field space, we can omit terms  $\propto (\beta m)^n$  with  $n > 4$  in Eqs. (155,156). Up to an additive ( $T$ -dependent, but  $\phi_c$ -independent) constant, the effective potential then has the approximate form,

$$V_{\text{eff},T} \approx \frac{1}{2} (m^2 + aT^2) \phi_c^2 - \frac{bT}{3} \phi_c^3 + \frac{\lambda + c}{4} \phi_c^4 + \dots \quad (157)$$

The coefficients  $a$ ,  $b$  and  $c$  sum the contributions from the SM plasma d.o.f.s:

$$a = \frac{1}{12} \left( \sum_{i=\text{boson}} g_i \frac{m_i^2}{\phi_c^2} + \frac{1}{2} \sum_{i=\text{fermion}} g_i \frac{m_i^2}{\phi_c^2} \right) \approx \frac{6m_W^2 + 3m_Z^2 + 6m_t^2}{12v^2}, \quad (158)$$

$$b = \frac{1}{4\pi} \sum_{i=\text{boson}} g_i \frac{m_i^3}{\phi_c^3} \approx \frac{6m_W^3 + 3m_Z^3}{4\pi v^3}, \quad (159)$$

$$c = \frac{1}{16\pi^2} \left( \sum_{i=\text{fermion}} g_i \frac{m_i^4}{\phi_c^4} \ln \frac{m_i^2}{a_F^2 T^2} - \sum_{i=\text{boson}} g_i \frac{m_i^4}{\phi_c^4} \ln \frac{m_i^2}{a_B^2 T^2} \right) \approx \frac{12m_t^4 \ln \frac{m_t^2}{a_F^2 T^2} - 6m_W^4 \ln \frac{m_W^2}{a_B^2 T^2} - 3m_Z^4 \ln \frac{m_Z^2}{a_B^2 T^2}}{16\pi^2 v^4}. \quad (160)$$

For the fermions, we included only the top quark, with  $g_t = 12$  (4 Dirac states times 3 QCD colours). For the bosons, we included only the weak gauge bosons with  $g_W = 2 \times 3$  and  $g_Z = 3$  (3 polarization states, times 2 charge states for  $W^\pm$ ). We find  $a \approx 0.33$ ,  $b \approx 0.03$ ,  $c \approx -0.05$  (in  $c$  we used the reference value  $T = 200$  GeV).

Now, at very high  $T$ , the origin  $\phi_c = 0$  is locally stabilised, since at sufficiently high  $T$  it would always be true that  $m^2 + aT^2 > 0$  (recall that  $m^2$  is negative, approximately given by  $m^2 \approx -\lambda v^2 \approx -m_h^2/2 \approx -88 \text{ GeV}^2$ ). The origin ceases to be stabilized when the temperature drops below the value

$$T_0^2 \approx \frac{-m^2}{a} \approx (154 \text{ GeV})^2. \quad (161)$$

In the SM,  $T_0$  is a reasonable and rather robust estimate for the actual temperature of SSB.

However, to the extent that the approximate expression of Eq. (157) can be trusted in detail, due to the (small) negative cubic term a remote minimum should appear slightly before the origin is locally destabilised. At  $T_c$ , given by

$$T_c^2 \approx \frac{(\lambda + c)a}{(\lambda + c)a - \frac{b^2}{9}} T_0^2 \approx 1.004 T_0^2, \quad (162)$$

the remote minimum would become degenerate with the minimum at the origin. Therefore, this simple analysis would suggest that in the SM, SSB *might* proceed via a first-order PT, provided that the tunnelling to the remote barrier could commence efficiently in the very short time interval it takes the Universe to cool from  $T_c \approx 1.004 T_0$  down to  $T_0$ .

In practice, the conclusion one might arrive at from this analysis, that the SM has a (numerically fragile) window of opportunity for an exciting first-order EWPT, is premature. When analysing the EWPT using more rigorous QFT methods, we will be able to see that the thermal potential we considered up until now corresponds to the one-loop approximation in the QFT loop expansion. Then, we will also see that for the SM, higher order loop corrections destroy the validity of the one-loop analysis in the region of  $T$  and field space from which the 1st order PT derived; the fragile 1st order PT is thus an illusion: lattice field theory computations demonstrate that the SM EWPT is a smooth crossover, occurring near  $T \approx T_0$ .

There is an easy (but rough) rule of thumb that one can use to check if the thermal cubic barrier is real, or an artefact of perturbation theory. To derive it, consider the thermal fluctuation in  $\phi$ , treating  $\varphi$  as massless for this purpose. Using the tools that we will derive in Sec. IV A 2:

$$\delta\phi_T^2 \approx \frac{T^2}{12}. \quad (163)$$

To check if the thermal cubic-generated barrier is real, we can compare the field at which the barrier peaks during  $T = T_c$  to the thermal fluctuation. At  $T = T_c$ , the barrier peaks at

$$\phi_p \approx T_c \left( 1 - \frac{T_0^2}{T_c^2} \right) \frac{a(\lambda + c)}{4b} = \frac{b}{36} T_c. \quad (164)$$

The barrier might be real, therefore, if

$$\phi_p^2 > \frac{T_c^2}{12} \quad \leftrightarrow \quad b > \frac{36}{\sqrt{12}} \approx 10.4. \quad (165)$$

For the SM,  $b \ll 1$ , and the condition in Eq. (165) is badly false. The thermal barrier in the SM is therefore indeed a mirage.

In terms of model-building beyond the SM, it is not difficult to construct models with a robust first order PT, even without the effect of bosonic d.o.f. in the plasma. For instance, a tree-level scalar field potential of the form  $V(\phi) = a\phi^2 + b\phi^3 + c\phi^4 + \dots$ , could easily have a hefty barrier between a symmetric minimum at the origin and an SSB minimum further away. This can also be achieved with sufficiently many light bosonic d.o.f., that could produce a numerically robust thermal cubic term; models of this type were notably considered in the context of low-scale supersymmetry. In practice, to my personal taste, the model-building in such plasma d.o.f. constructions usually seems ad-hoc and fine-tuned.

## 2. Symmetry restoration: canonical quantization

Canonical quantization offers a derivation of the thermal potential, that is easy to generalise to non-thermal states of the background plasma.

Consider the classical EOM for a scalar field  $\phi$  in FRW background,

$$\frac{1}{\sqrt{-g}} \frac{\partial}{\partial x^\mu} \left( \sqrt{-g} g^{\mu\nu} \frac{\partial \phi}{\partial x^\nu} \right) + \frac{\partial V_0}{\partial \phi} = 0. \quad (166)$$

We would like to see how quantum effects modify the classical EOM. To calculate this, we split the field into a classical background part and a fluctuation part,

$$\phi = \phi_c + \varphi. \quad (167)$$

By assumption in Eq. (167), we have  $\langle \varphi \rangle = 0$ , and  $\langle \phi \rangle = \phi_c$ . We will quantize  $\varphi$  using canonical quantization, and check the effect on the dynamics of  $\phi_c$  in the presence of some state specified in terms of particle excitations of  $\varphi$ .

Plugging Eq. (167) into Eq. (166), expanding in powers of  $\varphi$ , and taking the expectation value of the result, gives

$$\frac{1}{\sqrt{-g}} \frac{\partial}{\partial x^\mu} \left( \sqrt{-g} g^{\mu\nu} \frac{\partial \phi_c}{\partial x^\nu} \right) + \frac{\partial V_0(\phi_c)}{\partial \phi_c} + \frac{1}{2} \frac{\partial^3 V_0(\phi_c)}{\partial \phi_c^3} \langle \varphi^2 \rangle = 0, \quad (168)$$

where higher powers of  $\varphi$  were neglected. Our task therefore boils down to calculating  $\langle \varphi^2 \rangle$ . We will carry this out assuming that the spacetime dynamics (dynamics of  $g_{\mu\nu}$ ) is slow and negligible, and can be taken into account in an adiabatic approximation. In addition, we will assume weak couplings and neglect self-interaction of the  $\varphi$  fluctuation with itself. The EOM solved by  $\varphi$  is then

$$\frac{1}{\sqrt{-g}} \frac{\partial}{\partial x^\mu} \left( \sqrt{-g} g^{\mu\nu} \frac{\partial \varphi}{\partial x^\nu} \right) + m_\varphi^2(\phi_c) \varphi \approx 0, \quad (169)$$

where

$$m_\varphi^2 = \frac{\partial^2 V_0(\phi_c)}{\partial \phi_c^2}. \quad (170)$$

Canonical quantization of  $\varphi$  can be done as usual,

$$\varphi(t, \mathbf{x}) = \int \frac{d^3 \mathbf{q}}{(2\pi)^3 \sqrt{2\omega_q}} (e^{-iqx} a_{\mathbf{q}} + e^{iqx} a_{\mathbf{q}}^\dagger), \quad (171)$$

with

$$[a_{\mathbf{p}}, a_{\mathbf{p}'}^\dagger] = (2\pi)^3 \delta^{(3)}(\mathbf{p} - \mathbf{p}'). \quad (172)$$

As a first step, before considering an excited state, we do the calculation in the empty Minkowski vacuum state. The Minkowski vacuum state  $|0\rangle$  is specified to obey

$$a_{\mathbf{p}}|0\rangle = 0. \quad (173)$$

Under the empty vacuum, we have:

$$\langle 0|\varphi^2|0\rangle = \int \frac{d^3 \mathbf{q}}{(2\pi)^3 2\omega_q} = \frac{1}{2} \int \frac{d^3 \mathbf{q}}{(2\pi)^3} \frac{1}{\sqrt{m_\varphi^2 + \mathbf{q}^2}}. \quad (174)$$

Thus,

$$\begin{aligned} \frac{1}{2} \frac{\partial^3 V_0(\phi_c)}{\partial \phi_c^3} \langle \varphi^2 \rangle &= \frac{1}{2} \frac{\partial m_\varphi^2}{\partial \phi_c} \left( \frac{1}{2} \int \frac{d^3 \mathbf{q}}{(2\pi)^3} \frac{1}{\sqrt{m_\varphi^2 + \mathbf{q}^2}} \right) = \frac{1}{2} \frac{\partial m_\varphi^2}{\partial \phi_c} \frac{\partial}{\partial m_\varphi^2} \int^{m_\varphi^2} dm^2 \left( \frac{1}{2} \int \frac{d^3 \mathbf{q}}{(2\pi)^3} \frac{1}{\sqrt{m^2 + \mathbf{q}^2}} \right) \\ &= \frac{\partial}{\partial \phi_c} \int \frac{d^3 \mathbf{q}}{(2\pi)^3} \frac{\sqrt{m_\varphi^2 + \mathbf{q}^2}}{2} \equiv \frac{\partial}{\partial \phi_c} V_1(\phi_c). \end{aligned} \quad (175)$$

The correction term  $V_1$  is thus precisely equal to the usual  $\int \frac{\omega}{2}$  vacuum energy density of the QFT. The effective potential  $V_{\text{eff}} = V_0 + V_1$  we obtain this way coincides with what we found in the path integral formalism, in Sec. II A.

**What changes if the background state contains  $\varphi$  particle excitations?** The excited background state  $|\Omega\rangle$  can be specified via

$$\langle \Omega | a_{\mathbf{p}}^\dagger a_{\mathbf{p}'} | \Omega \rangle = (2\pi)^3 \delta^{(3)}(\mathbf{p} - \mathbf{p}') f_{\mathbf{p}}, \quad \langle \Omega | a_{\mathbf{p}}^\dagger a_{\mathbf{p}'}^\dagger | \Omega \rangle = \langle \Omega | a_{\mathbf{p}} a_{\mathbf{p}'} | \Omega \rangle = 0, \quad (176)$$

where  $f_{\mathbf{p}}$  is a phase space distribution function. Using this definition together with the usual commutation relations under the integral, the expectation value of  $\varphi^2$  in the excited state is:

$$\langle \Omega | \varphi^2 | \Omega \rangle = \int \frac{d^3 \mathbf{q}}{(2\pi)^3 \omega_q} \left( \frac{1}{2} + f_{\mathbf{q}} \right). \quad (177)$$

The first term in the bracket in Eq. (177) gives the vacuum contribution  $V_1$  as before. The second term is due to the background particle excitations. If the background is thermal with

temperature  $T$ , we can use Eq. (152). The new contribution to the last term of Eq. (168) is

$$\begin{aligned}
\frac{1}{2} \frac{\partial^3 V_0(\phi_c)}{\partial \phi_c^3} \langle \varphi^2 \rangle_T &= \frac{1}{2} \frac{\partial m_\varphi^2}{\partial \phi_c} \int \frac{d^3 \mathbf{q}}{(2\pi)^3 \omega_q} f_{\mathbf{q}} = \frac{1}{2} \frac{\partial m_\varphi^2}{\partial \phi_c} \frac{\partial}{\partial m_\varphi^2} \int^{m_\varphi^2} dm^2 \int \frac{d^3 \mathbf{q}}{(2\pi)^3} \frac{f_{\mathbf{q}}}{\omega_q} \\
&= \frac{\partial}{\partial \phi_c} \frac{1}{2} \int \frac{d^3 \mathbf{q}}{(2\pi)^3} \int^{m_\varphi^2} \frac{dm^2}{\sqrt{m^2 + \mathbf{q}^2}} \frac{1}{e^{\beta \sqrt{m^2 + \mathbf{q}^2}} \pm 1} \\
&= \frac{\partial}{\partial \phi_c} \frac{T^4}{2\pi^2} \int dx x^2 \int^{\beta^2 m_\varphi^2} \frac{dz}{2\sqrt{z+x^2}} \frac{1}{e^{\sqrt{z+x^2}} \pm 1} \\
&= \frac{\partial}{\partial \phi_c} (\mp 1) \frac{T^4}{2\pi^2} \int_0^\infty dx x^2 \ln \left( 1 \pm e^{-\sqrt{\beta^2 m_\varphi^2 + x^2}} \right) = \frac{\partial}{\partial \phi_c} V_T(\phi_c). \quad (178)
\end{aligned}$$

(In our current scalar field example, we should take the BE distribution with  $(-)$  in the log; but I have generalised the calculation a bit and Eq. (178) applies to both bosonic and fermionic particles.) Comparing to Eq. (154), we see that we have rederived the thermodynamic result  $V_T = -p$ .

*a. Going beyond a thermal background.* The canonical quantization method offers a direct and intuitively clear way to consider the effect of a finite-density background state that is not necessarily thermal: all we need to do, is replace the thermal distribution function by a different form of  $f_{\mathbf{q}}$ , and re-evaluate Eq. (178).

As an interesting example, suppose that we are interested in the effect of a background density of particles, that are assumed to have been in a maximum entropy thermal equilibrium distribution early on in the cosmic evolution of the Universe, but that have since then decoupled from the rest of the plasma, with decoupling occurring sufficiently early such that at the epoch of the decoupling, the particles were still highly relativistic. The late-time distribution function of such decoupled (and thus, out-of-equilibrium) particles is given by the BE or FD distribution, but with energy  $\omega$  replaced by momentum:

$$f_q^{(\text{dec})} = \frac{1}{e^{\beta |\mathbf{q}|} \pm 1}, \quad (179)$$

where  $\beta = 1/T$  is the redshift-dependent temperature parameter. (If decoupling occurred at a redshift  $z_{\text{dec}}$  when  $T = T_{\text{dec}}$ , then  $T(z) = \frac{1+z}{1+z_{\text{dec}}} T_{\text{dec}}$ .) Importantly, notice that  $f_{\mathbf{q}}^{(\text{dec})}$  is independent of the particle energy, so it does not depend on the particle mass  $m_\varphi$  or on  $\phi_c$ .

Using our formalism, in this example we find:

$$\begin{aligned}
\frac{1}{2} \frac{\partial^3 V_0(\phi_c)}{\partial \phi_c^3} \langle \varphi^2 \rangle_{T,\text{dec}} &= \frac{1}{2} \frac{\partial m_\varphi^2}{\partial \phi_c} \frac{\partial}{\partial m_\varphi^2} \int \frac{d^3 \mathbf{q}}{(2\pi)^3} f_{\mathbf{q}}^{(\text{dec})} \int^{m_\varphi^2} dm^2 \frac{1}{\omega_q} \\
&= \frac{\partial}{\partial \phi_c} \int \frac{d^3 \mathbf{q}}{(2\pi)^3} f_{\mathbf{q}}^{(\text{dec})} \int^{m_\varphi^2} \frac{dm^2}{2\sqrt{m^2 + \mathbf{q}^2}} \\
&= \frac{\partial}{\partial \phi_c} \int \frac{d^3 \mathbf{q}}{(2\pi)^3} f_{\mathbf{q}}^{(\text{dec})} \sqrt{m_\varphi^2 + \mathbf{q}^2} = \frac{\partial}{\partial \phi_c} V_{T,\text{dec}}(\phi_c). \quad (180)
\end{aligned}$$

Inspection of this result shows that

$$V_{T,\text{dec}}(\phi_c) = \rho(\phi_c). \quad (181)$$

That is, when the background state is dynamically decoupled from the field  $\phi_c$  – in the sense that the phase space distribution function  $f_{\mathbf{q}}$  is independent of  $\phi_c$  – the corresponding correction to the effective potential becomes just the *energy density*,  $\rho$ , of the background gas, rather than



negative the pressure,  $-p$ , of the gas, which was what we obtained if the gas distribution function is thermal and adjusts itself as a function of  $\phi_c$  via the particle mass  $m_\varphi(\phi_c)$ .

For the decoupled gas of Eq. (179), however, the entropy density is independent of  $\phi_c$ : it simply counts the states which are a legacy of an earlier epoch of thermal equilibrium, but which have decoupled and no longer react to external sources. The  $\phi_c$ -dependent part of  $F$  is then simply  $\rho$  (additional  $\phi_c$ -independent terms are not determined in our calculation: we reconstructed  $V_{\text{eff}}$  here only through its derivative  $\frac{\partial V_{\text{eff}}}{\partial \phi_c}$ ).

### 3. Symmetry restoration: path integral formalism

In Sec. II A, to study SSB in a vacuum background state that is free of particle excitations, we noted that the expectation value of the field could be obtained from (we set  $\hbar = 1$ )

$$\langle \phi(x) \rangle_J = \frac{\delta W[J]}{\delta J(x)} = \frac{\int [D\phi] \phi(x) e^{i(S[\phi] + \phi J)}}{\int [D\phi] e^{i(S[\phi] + \phi J)}} \equiv \bar{\phi}_J(x), \quad (182)$$

using the generating functional of connected Greens functions

$$W[J] = -i \ln Z[J] \quad \leftrightarrow \quad Z[J] = e^{iW[J]}, \quad (183)$$

based on the path integral

$$Z[J] = \mathcal{N} \int [D\phi] e^{i(S[\phi] + \phi J)}. \quad (184)$$

It will be useful to recall that  $Z[J]$  is the path integral representation of the vacuum-to-vacuum amplitude (in the presence of the source  $J$ )<sup>24</sup>,

$$\mathcal{N} \int [D\phi] e^{i(S[\phi] + \phi J)} = \lim_{\mathcal{T} \rightarrow \infty} \text{tr} e^{-iHT(1-i\epsilon)} e^{i\phi J} = \lim_{\mathcal{T} \rightarrow \infty} \langle \Omega | e^{-iHT(1-i\epsilon)} e^{i\phi J} | \Omega \rangle, \quad (185)$$

We need to introduce a small negative imaginary part  $-i\epsilon$  to ensure that the external state is projected onto the ground state – the vacuum<sup>25</sup>  $|\Omega\rangle$ . On the leftmost side of Eq. (185), the  $\mathcal{T}$  dependence is located in the boundary condition of the time integral in the exponent:

$$S[\phi] + \phi J = \int_{-\frac{\mathcal{T}}{2}}^{\frac{\mathcal{T}}{2}} dt \int d^3\mathbf{x} (\mathcal{L}(\phi, \partial_\mu \phi) + \phi J). \quad (186)$$

The 1-loop piece of the effective action came from approximating  $Z[J]$  by expanding  $S[\phi]$  around the classical VEV  $\phi_c$ , and calculating the functional determinant, encapsulating variations  $\varphi$  around  $\phi_c$  via  $\phi = \phi_c + \varphi$ . The 1-loop piece of the effective action read  $\Gamma_1 = \frac{i}{2} \ln \text{Det} \left( -\frac{\delta^2 S}{\delta \phi_c^2} \right)$ , where the second variation of the action was given by the differential operator  $-\frac{\delta^2 S}{\delta \phi_c^2} = \partial_t^2 - \nabla^2 + m_\phi^2$ . The boundary conditions for the eigenvalue problem were that the eigenfunctions  $f_\lambda(x)$  vanish on the boundary of  $D = 3 + 1$  spacetime; but the details of the behaviour on the boundary were actually not important, because we took the 3-volume to

<sup>24</sup> We use curly  $\mathcal{T}$  to denote a real time parameter, because we here we keep  $T$  for temperature.

<sup>25</sup> See, e.g., Peskin & Schroeder, Ch.9.2.

infinity in the continuum limit, and also took  $\mathcal{T} \rightarrow \infty$ .

Our goal now is to extend the results of Sec. II A to the case in which the background “vacuum” state contains a gas of particles in a thermal state.

A thermal state corresponds to an incoherent ensemble, where every possible Hamiltonian eigenstate of the QFT participates with a probability weight given by  $e^{-\beta H}$ . The thermal statistical expectation value of some operator  $\mathcal{O}$  is given by the thermal average,

$$\langle \mathcal{O} \rangle_T = \frac{\text{tr} e^{-\beta H} \mathcal{O}}{\text{tr} e^{-\beta H}}. \quad (187)$$

To incorporate this thermal averaging procedure in the SSB analysis, we should replace the quantum vacuum-to-vacuum expectation value in Eq. (185) by the thermal expectation value. Thus, we define the thermal generating functional as:

$$Z_T[J] = \text{tr} e^{-\beta H} e^{i\phi J}. \quad (188)$$

We also define the functional  $W_T[J]$  in the usual way,

$$W_T[J] = -i \ln Z_T[J]. \quad (189)$$

With this, the thermal VEV is given by

$$\langle \phi \rangle_{T,J} = \frac{\delta W_T}{\delta J} = \frac{\text{tr} e^{-\beta H} \phi e^{i\phi J}}{\text{tr} e^{-\beta H}}. \quad (190)$$

This construction reveals that the finite- $T$  VEV is given by a closely related procedure to the zero- $T$  VEV: we can implement it by setting, in the RHS of Eq. (185),

$$\mathcal{T} = -i\beta. \quad (191)$$

In the path integral formulation, the only place in which this replacement enters is, again, in the boundary condition of the time integral in the action. When we compute the 1-loop correction in the saddle point approximation, this becomes a boundary condition for the eigenvalue problem in the functional determinant. Specifically, we must extremise

$$iS[\phi] = i \int_{-\frac{i\beta}{2}}^{\frac{-i\beta}{2}} dt \int d^3\mathbf{x}^3 \mathcal{L}(\phi, \partial_t \phi) = -S_E[\phi] = - \int_{-\frac{\beta}{2}}^{\frac{\beta}{2}} d\tau \int d^3\mathbf{x} \mathcal{L}_E(\phi, \partial_\tau \phi). \quad (192)$$

Referring back to our computations in Secs. II A and III B, and jumping directly to Euclidean signature, the functional determinant we need to evaluate requires that we find the eigenfunctions  $f_n(x)$  satisfying

$$(-\nabla_E^2 + m_\phi^2) f_\lambda(x) = \lambda f_\lambda(x), \quad (193)$$

where  $\nabla_E^2 = \partial_\tau^2 + \vec{\nabla}^2$ , in which we now need to impose the boundary condition  $f_\lambda(0, \mathbf{x}) = f_\lambda(\beta, \mathbf{x})$ . This problem is the finite- $T$  analog of Eq. (27) (and the closely related Eq. (117)).

The eigenfunctions are quasi-periodic:  $f_{n,\mathbf{k}} = e^{i\frac{2\pi n}{\beta} \tau - i\mathbf{k}\mathbf{x}}$ , with eigenvalue  $\lambda = \frac{(2\pi n)^2}{\beta^2} + \mathbf{k}^2 + m_\phi^2$ . The 1-loop correction is, then:

$$\Gamma_{1,T} = \frac{i}{2} \ln \text{Det} \left( -\frac{\delta^2 S}{\delta \phi_c^2} \right)_T = -\frac{V_3}{2} \sum_{n=-\infty}^{\infty} \int \frac{d^3\mathbf{k}}{(2\pi)^3} \ln \left( \frac{(2\pi n)^2}{\beta^2} + \mathbf{k}^2 + m_\phi^2 \right), \quad (194)$$

where  $V_3$  is the 3D spatial volume of spacetime. Let us define the effective volume factor<sup>26</sup>,

$$V_{U,T} = V_3\beta. \quad (195)$$

In terms of this effective 4-volume, we can factor out the effective potential as usual (for homogeneous  $\phi_c$ ):

$$\Gamma_{1,T} = -V_{U,T}V_{1,T}(\phi_c). \quad (196)$$

The 1-loop piece of the finite- $T$  effective potential is, then:

$$V_{1,T} = \frac{1}{2\beta} \sum_{n=-\infty}^{\infty} \int \frac{d^3\mathbf{k}}{(2\pi)^3} \ln \left( \frac{(2\pi n)^2}{\beta^2} + \omega_{\mathbf{k}}^2 \right), \quad (197)$$

where as usual we define  $\omega_{\mathbf{k}} = \sqrt{\mathbf{k}^2 + m_\phi^2}$ .

To evaluate  $V_{1,T}$ , we can use the fact that we are only interested in the field-dependent part of the expression. Thus we can insert  $\int d\omega_{\mathbf{k}}^2 \frac{\partial}{\partial \omega_{\mathbf{k}}^2}$  under the  $\mathbf{k}$  integral, to obtain<sup>27</sup>,

$$\begin{aligned} V_{1,T} &= \int \frac{d^3\mathbf{k}}{(2\pi)^3} \int d\omega_{\mathbf{k}}^2 \frac{\partial}{\partial \omega_{\mathbf{k}}^2} \frac{1}{2\beta} \sum_{n=-\infty}^{\infty} \ln \left( \frac{(2\pi n)^2}{\beta^2} + \omega_{\mathbf{k}}^2 \right) + \text{Const} \\ &= \int \frac{d^3\mathbf{k}}{(2\pi)^3} \frac{1}{2\beta} \int d\omega_{\mathbf{k}}^2 \sum_{n=-\infty}^{\infty} \frac{1}{\frac{(2\pi n)^2}{\beta^2} + \omega_{\mathbf{k}}^2} \\ &= \int \frac{d^3\mathbf{k}}{(2\pi)^3} \frac{1}{2\beta} [\beta\omega_{\mathbf{k}} + 2 \ln(1 - e^{-\beta\omega_{\mathbf{k}}})] + \text{Const}. \end{aligned} \quad (198)$$

We can recognise the zero- $T$  piece:  $V_1 = \int \frac{d^3\mathbf{k}}{(2\pi)^3} \frac{\omega_{\mathbf{k}}}{2} + \text{Const}$ . The remaining field-dependent piece is, therefore, the finite- $T$  correction:  $V_T = T \int \frac{d^3\mathbf{k}}{(2\pi)^3} \ln(1 - e^{-\beta\omega_{\mathbf{k}}}) = \frac{T^4}{2\pi^2} \int dx x^2 \ln(1 - e^{-\sqrt{\beta^2 m_\phi^2 + x^2}})$ . Indeed, this coincides with Eq. (150), using the last line of Eq. (154) to express the pressure.

We have only done this derivation for scalar field theory, and so our expression corresponds to a gas of scalar particles. The generalisation to fermion fields follows similar lines, and can be found in, e.g., Quiros, M., hep-ph/9901312.

---

<sup>26</sup> It is interesting to note that the zero- $T$  procedure naturally yields the zero- $T$  effective potential as an energy density in an infinite 4D spacetime volume  $V_U$ , such that the dimensionless effective action is given by the product  $\Gamma_1 = -V_U V_1$ . In comparison, the thermal field theory construction yields the potential as energy density in 3D infinite spatial volume times a finite interval  $\beta$  in what would otherwise have been the time direction, that is, in  $V_{U,T}$ ; such that  $\Gamma_{1,T} = -V_{U,T} V_{1,T}$ . In general, at any value of  $T$ , the SSB VEV is found by minimizing the potential energy density  $V_{\text{eff}} = V_0 + V_{1,T} = V_0 + V_1 + V_T$ . (KB thanks [Abhishek Banerjee](#) for a discussion on this point.)

<sup>27</sup> We are using:  $\sum_{n=-\infty}^{\infty} \frac{1}{n^2 + a^2} = \frac{\pi}{a} \coth a\pi$ .